CHAPTER 4 PRESENTATIONS AND DISCUSSIONS OF EXPERIMENTAL AND THEORETICAL RESULTS

4.1 DEFINITIONS OF QUANTITIES FOR PRESENTATIONS

Figure 4.1 shows sample time histories of displacement of shaking table, x_s; liquid free surface elevation at the end wall, η_o; and base shear force, F, with liquid sloshing at steady state in the horizontal shaking table experiment. Several quantities are defined as follows for the presentations of results.

Figure 4.1 Sample time histories of displacement of shaking table, x_s, liquid surface elevation near the end wall, η_o and base shear Force, F (Shaking table experiment under horizontal motion).

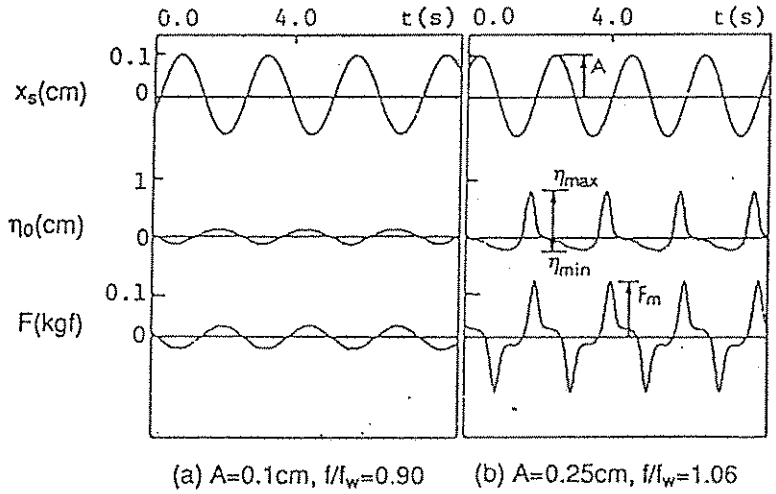

(a) A=0.1cm, f/f_w=0.90 (b) A=0.25cm, f/f_w=1.06

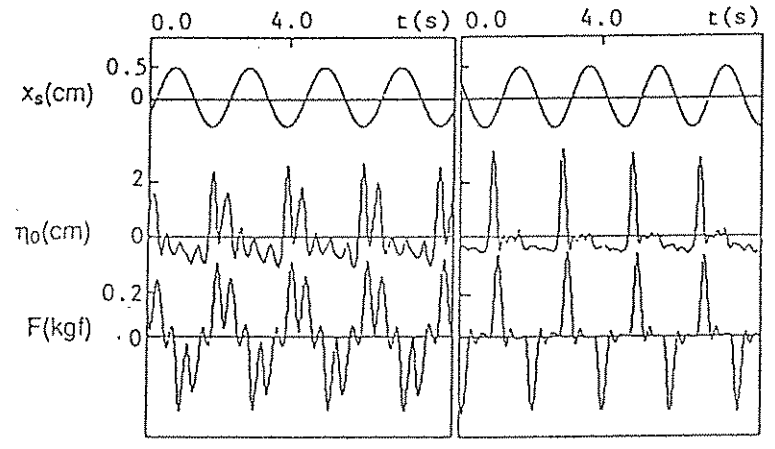

(c) A=0.5cm, f/f_w=1.06 (d) A=1.0cm, f/f_w=1.14

Dimensionless Maximum and Minimum Liquid Surface Elevation at the End Wall of TLD Tank. Liquid free surface elevation at the end wall of TLD tank, η_o equals 0 at still liquid free surface. During liquid sloshing, η_o has a maximum value η_{max} (wave crest) and a minimum value η_{min} (wave trough) in one cycle (Fig. 4.1). The dimensionless quantities η'_{max} and η'_{min} are defined as

$$\eta'_{max} = \eta_{max} / h; \qquad \eta'_{min} = \eta_{min} / h, \tag{4.1}$$

where h is liquid depth.

Dimensionless Amplitude Base Shear Force. Under a sinusoidal excitation, the base shear force $F(t)$ has the same amplitude F_m either in positive direction or negative direction (Fig. 4.1). F_m is nondimensionalized by the maximum inertia force of liquid treated as a solid mass in sinusoidal motion:

$$F'_m = F_m / (m_w \omega^2 A), \tag{4.2}$$

where $\omega = 2\pi f$, is the angular excitation frequency.

Dimensionless Energy Loss per Cycle. The shaking table inputs energy into the TLD, and the TLD itself dissipates energy, ΔE due to liquid sloshing. When TLD is at steady state, it means that in each cycle of excitation, the energy input into the TLD equals the energy dissipation inside the TLD. The energy input into the TLD, E_{input} can be calculated from the base shear force F and the displacement of shaking table x_s, which are both the functions of time. Thus the energy dissipation per cycle, ΔE can be calculated as

$$\Delta E = E_{input} = \int_t^{t+T} F(t)\, dx_s(t), \tag{4.3}$$

where T is the period of excitation, i.e. $2\pi/\omega$. From the above equation, we know that the energy dissipation per cycle depends both on the amplitudes of F and x_s and on the phase difference between them. ΔE is nondimensionalized as follows,

$$\Delta E' = \Delta E / (\frac{1}{2} m_w (\omega A)^2). \tag{4.4}$$

Note that $m_w(\omega A)^2/2$ is just a reference value to nondimensionalize but not the energy of liquid sloshing.

Response Amplitude of Structure attached with TLD. In TLD-sturcture interaction experiment, the response amplitude of structure attached with TLD

was measured. This quantity is employed for present the results of TLD-structure interaction, from which one can see the efficiency of TLD.

4.2 TLD SUBJECTED TO HORIZONTAL MOTION

4.2.1 Time Histories

The wave forms of these time histories vary as the excitation frequency or the base amplitude varies. Unsymmetrical wave form can be observed even under the harmonic excitation of small amplitude (Fig. 4.1b). At certain excitation frequencies, two or three waves can be observed in one cycle (e.g., Fig. 4.1c).

Figure 4.2 presents the measured transient time history responses of liquid surface elevation, η_0 and that of base shear force, F, for the input base amplitude $A = 0.25\ cm$. The wave forms of liquid motion vary as the excitation frequency changes. At $f/f_w = 1.001$, two waves in one cycle can be observed. This is a nonlinear effect of the second higher-harmonic of liquid sloshing, which is excited at an excitation frequency about one third of the natural frequency of second unsymmetrical mode of liquid sloshing. At $f/f_w = 0.951$, even the third higher-harmonic can be observed clearly. For shallow liquid sloshing in a rectangular tank, the natural frequencies are related as $\omega_2 \approx 3\omega_1$, $\omega_3 \approx 5\omega_1$ (ω_n: the natural frequencies of n^{th} higher-harmonics) (Eq.(2.25)). Near the fundamental resonance, quadratic nonlinearity and cubic nonlinearity induce coupling with the 2nd and the 3rd higher-harmonics, respectively, thereby changing the liquid sloshing qualitatively (Nayfeh and Mook 1979).

Numerical simulations corresponding to these cases are also shown for comparison. In numerical simulation, the liquid motion of TLD was assumed to be quiescent at $t=0$. The time increment was $1/60$ of the excitation period of shaking table. The computation was carried on until 80 periods where liquid sloshing was regarded to have reached steady state. Comparing the numerical simulation with the experimental results, good agreement can be seen. The TLD model developed here is satisfactory in predicting not only the fundamental resonance but also the nonlinearity which induces the effects of higher-harmonics of liquid sloshing.

Figure 4.3 shows some examples of force-displacement diagrams for the base displacement amplitude of $0.25\ cm$. One can find also in Fig. 4.3 that the simulation results agree well with those of the experiment.

Figure 4.2 The time histories of base shear force, F (Base amplitude A=0.25 cm).

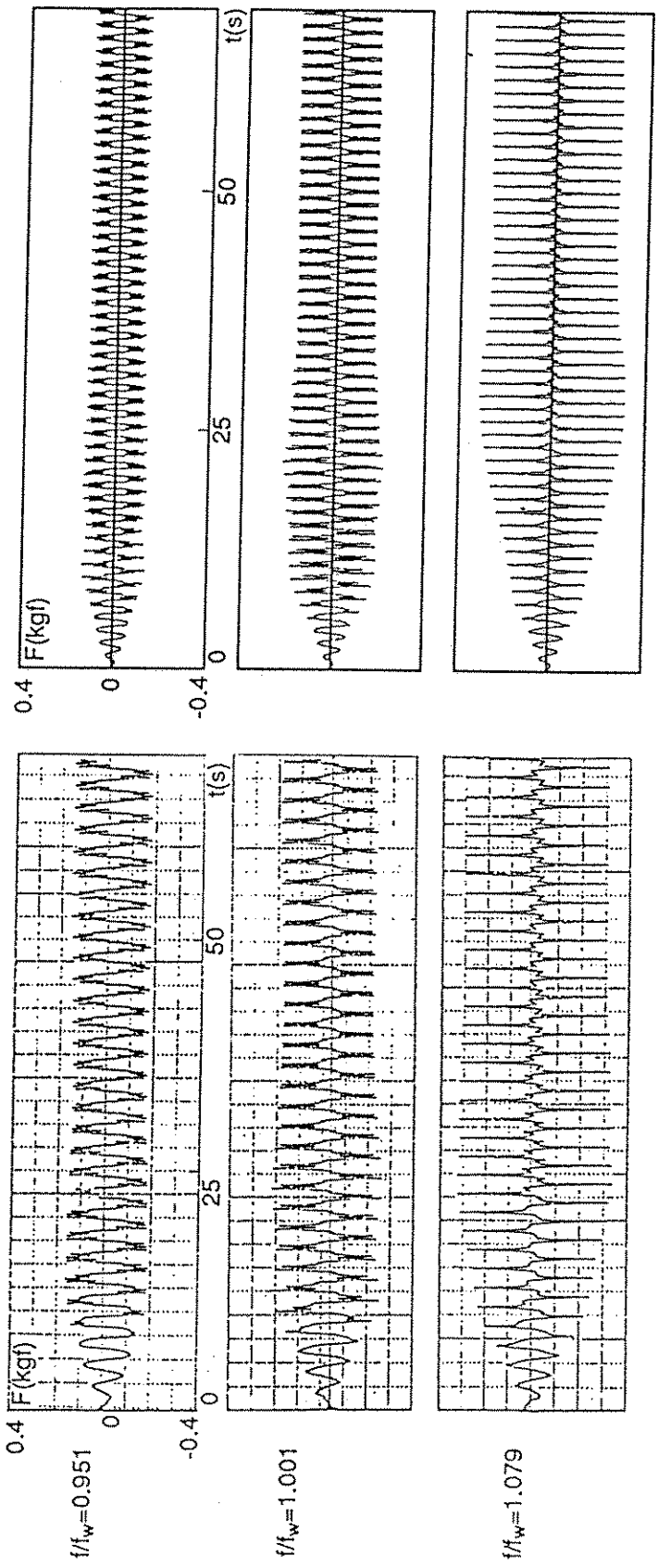

Figure 4.3 The energy dissipation loops (Base amplitude A=0.25 cm).

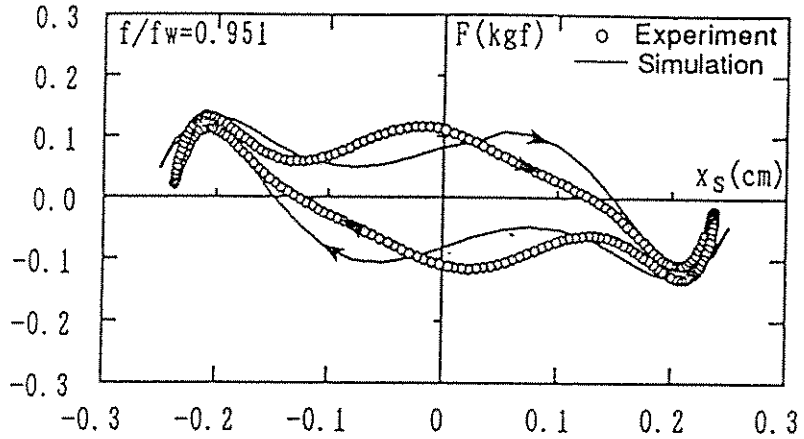

(a) f/f_w=0.951

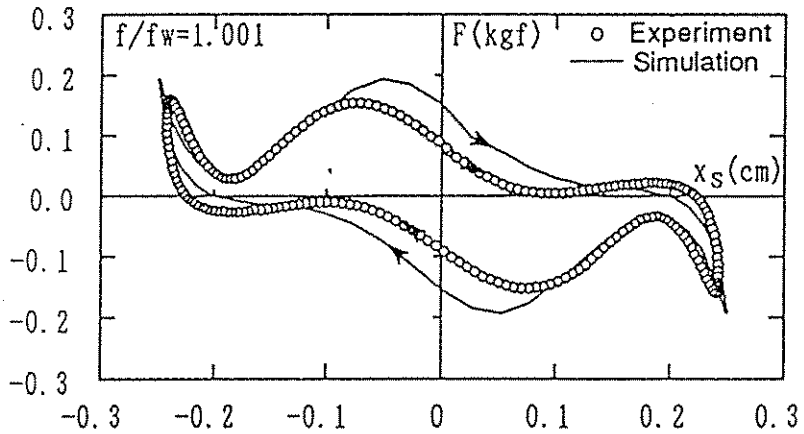

(b) f/f_w=1.001

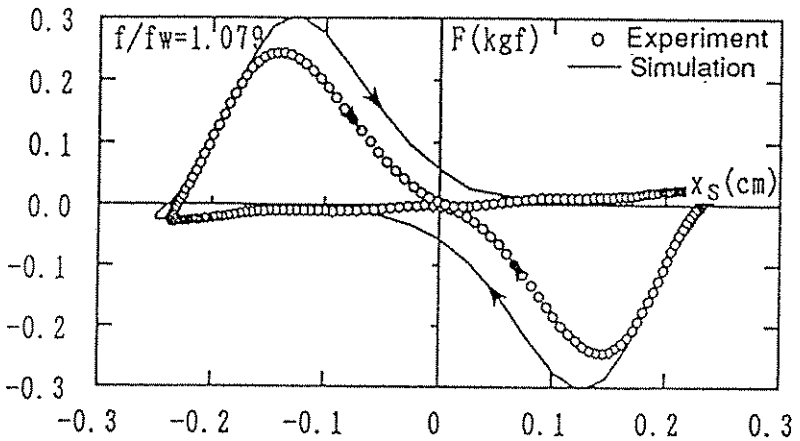

(c) f/f_w=1.079

Figure 4.4 Frequency responses of η'_{max} and η'_{min}, F'_m, and $\Delta E'$.

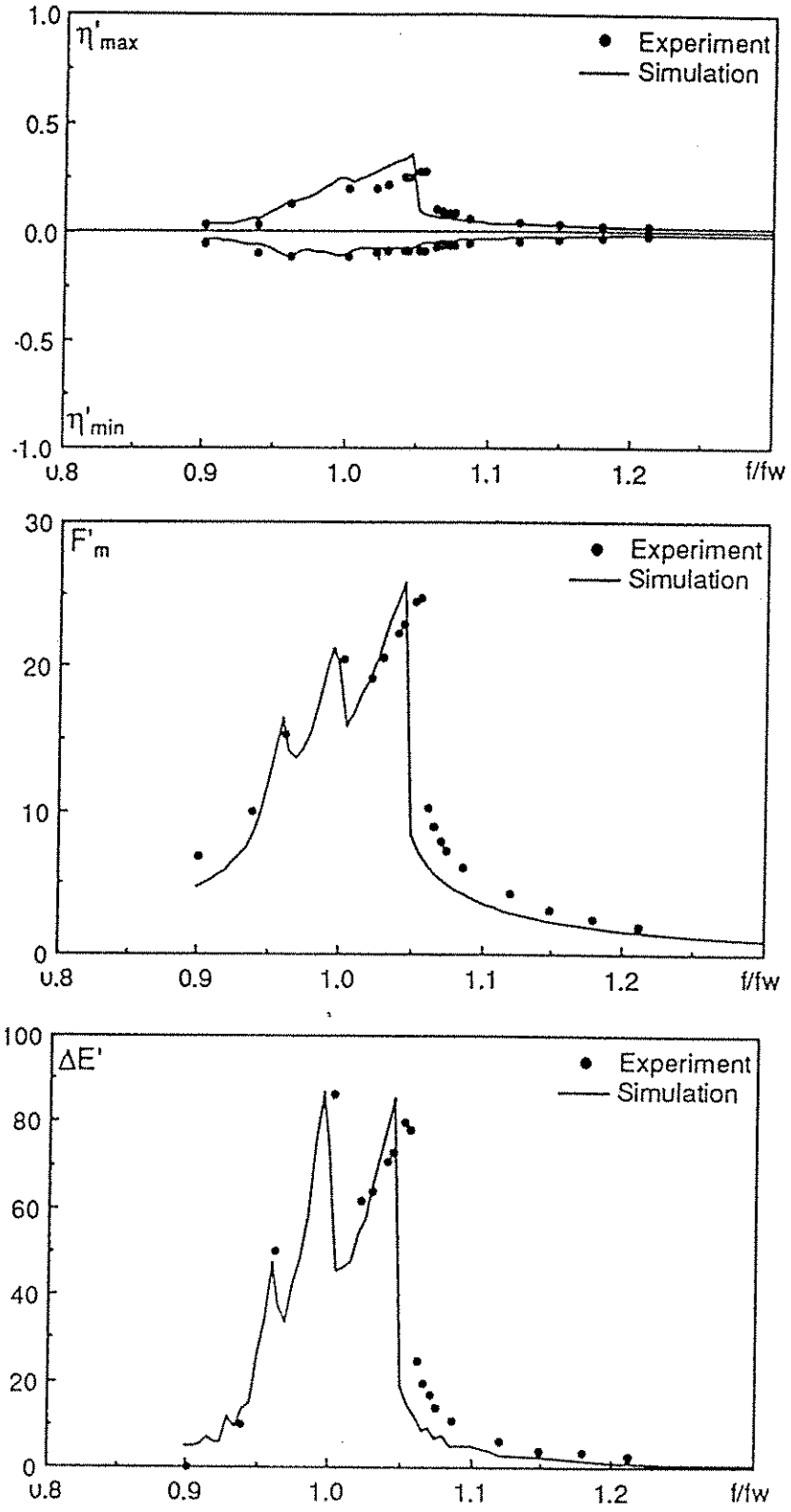

(a) Base Amplitude = 0.1 cm

Figure 4.4 (Continued).

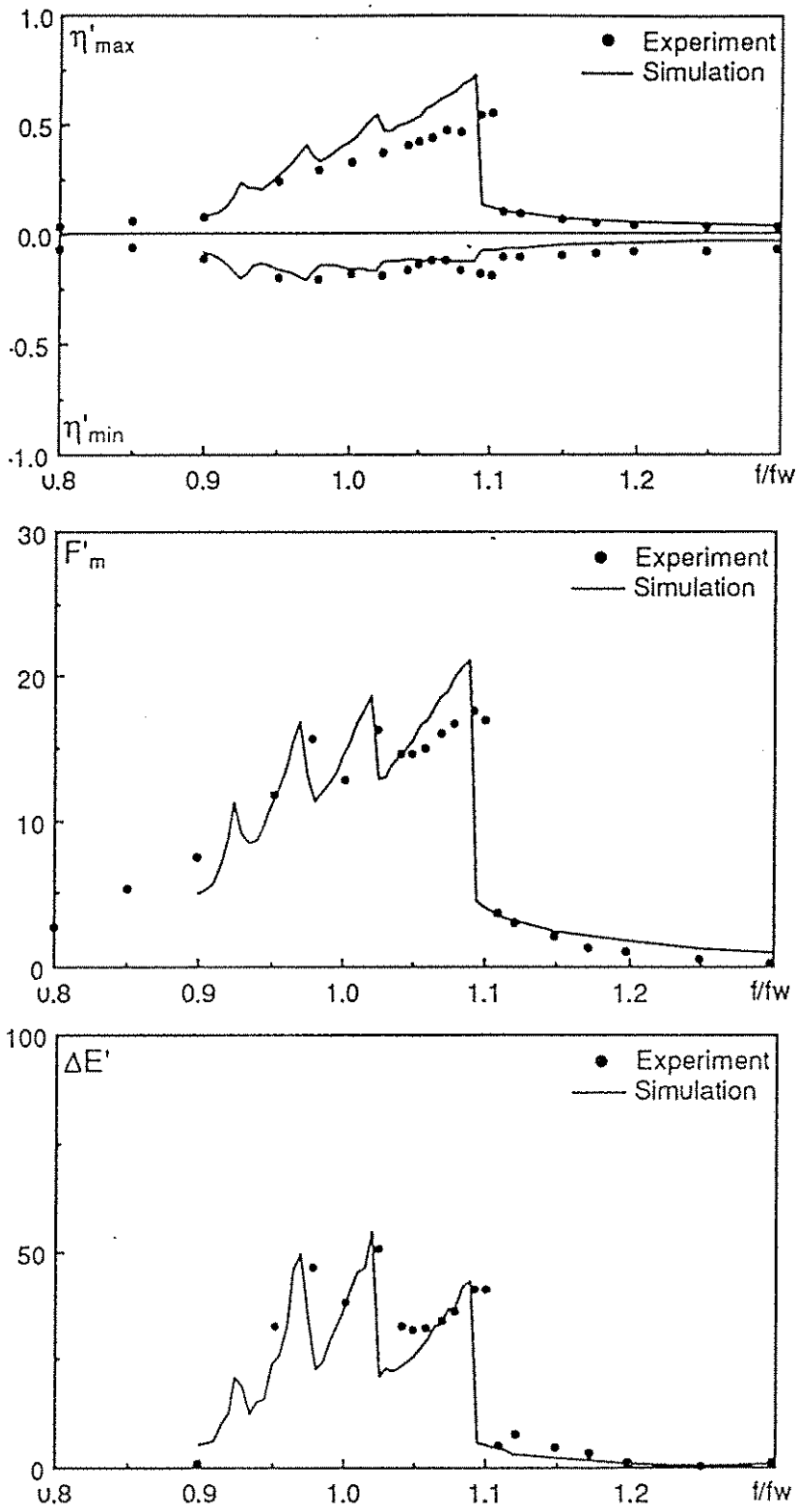

(b) Base Amplitude = 0.25 cm

Figure 4.4 (Continued).

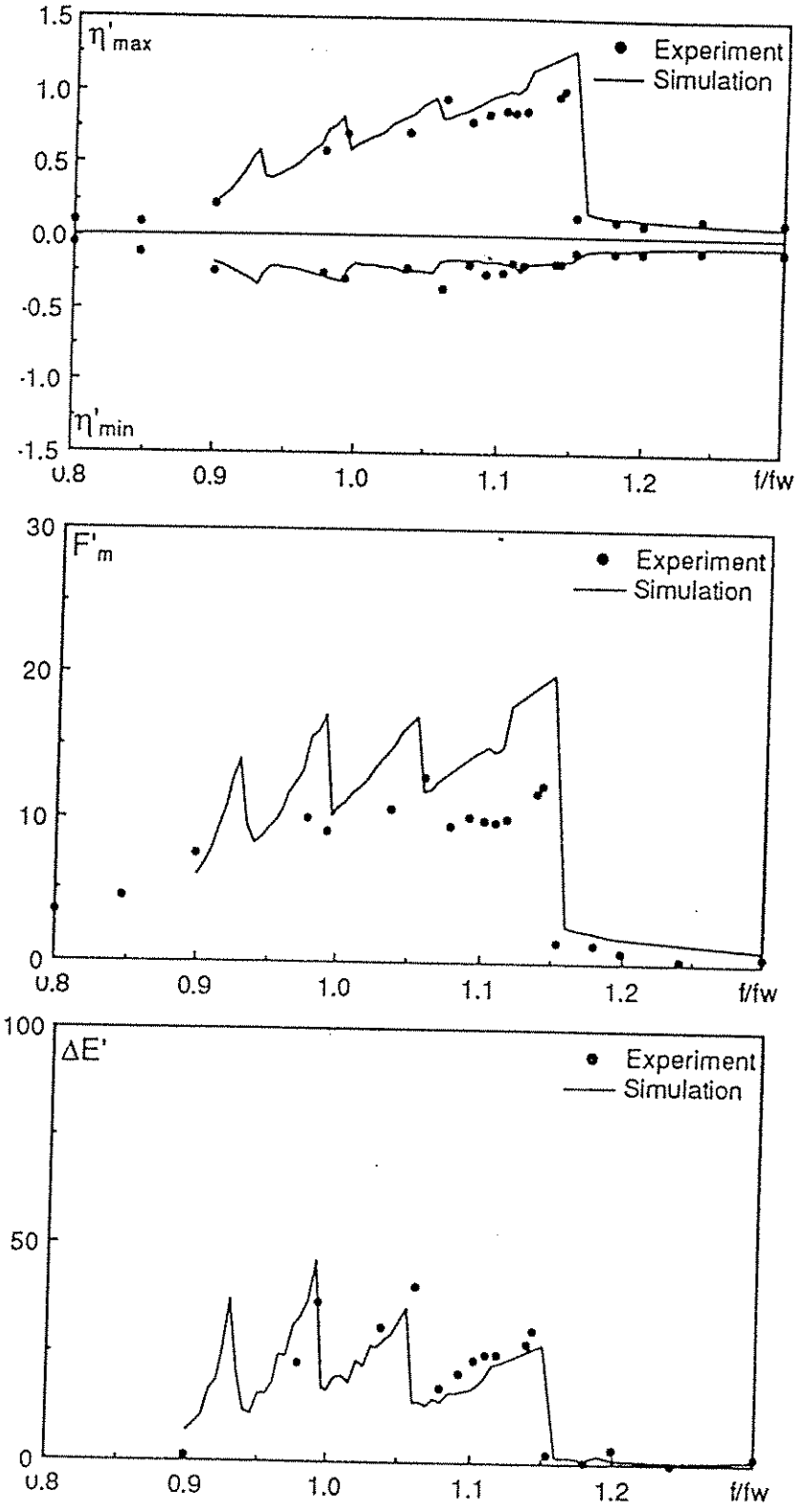

(c) Base Amplitude = 0.5 cm

Figure 4.4 (Continued).

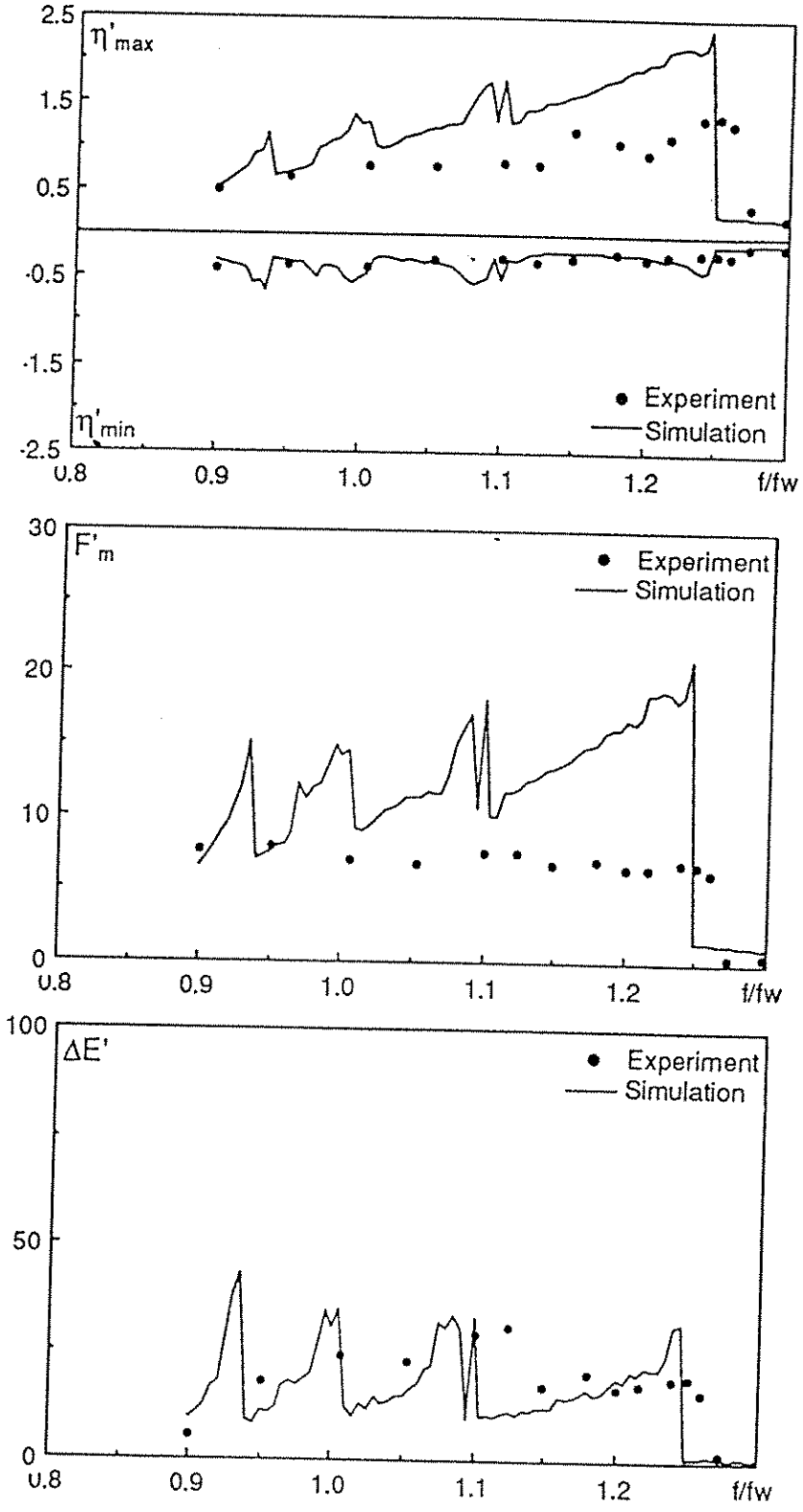

(d) Base Amplitude = 1.0 cm

4.2.1 Frequency Responses

In Fig.4.4, the nondimensionalized quantities, η'_{max} , η'_{min} (surface elevation), F'_m (maximum base shear force) and $\Delta E'$ (energy loss in TLD per cycle) are plotted for the frequency ratio range of $0.9 < f/f_w < 1.3$.

All of the cases in the experiment indicate that the liquid motions possess strong nonlinearity (Fig. 4.4a to d). The fundamental resonant frequency ratio is greater than *1.00* even for the smallest input amplitude case *(A = 0.1 cm)*. At a certain value of frequency ratio larger than *1.00*, η'_{max} and η'_{min} jumps, indicating that the nonlinearity of liquid sloshing is a "hardening spring" type. As the input amplitude increases, the resonant frequency becomes larger. The resonant frequency for the base amplitude of *0.1 cm* is about $1.1f_w$ and increases to about $1.25f_w$ for the base amplitude of *1.0 cm*. This indicates that the nonlinearity becomes stronger.

Local peaks of η'_{max} (and also of F'_m and $\Delta E'$) at the frequency range less than the fundamental resonant frequency, can be observed in Fig.4.4a, b and c. These are due to the appearance of higher harmonics as seen in Figs. 4.1 and 4.2.

For the relatively small amplitude excitation *(0.1 cm, 0.25 cm, 0.5 cm)*, the simulation can predict the experimental results well. For the input amplitude of *1.0 cm*, however, the wave height exceeded the liquid depth, *h* and the existences of breaking waves were also visually identified (Fig. 4.4d). In this case, the simulation results do not agree with those of the experiments. The simulation overestimates η'_{max} and F'_m, although the resonant frequency ratio is well predicted. It should be noticed in Fig. 4.4d that the simulation underestimates $\Delta E'$ in the range $1 < f/f_w < 1.25$. This is probably because the energy dissipation for the base displacement amplitude of *1.0 cm* or larger is due not only to viscosity of liquid but also to breaking waves. All these results indicate that the TLD model developed here is valid as far as the continuous free surface condition is satisfied. In further increases of the base amplitude, *A (>1.0 cm)*, η'_{max} , η'_{max} , F'_m and $\Delta E'$ did not show clear resonance peaks and became very flat over a wide range of f/f_w (Sun, et al. 1989).

In practice, the vibration amplitudes of structure may be in a range where breaking waves in TLD occur. To make the TLD model valid even in wave breaking condition, the model is modified. The modified model is found to be able to explain the experimental results well [Sun et al. 1990]. The details are given in Sections 2.4 and 5.4.

4.3 TLD SUBJECTED TO PITCHING MOTION

4.3.1 Time Histories

As a sample, the time histories of wave surface elevation near the end wall of the TLD tank are shown in Fig. 4.5 for the case R6N1-01 (Table 3.6) ($h=3.0cm$, $\theta_0=0.1\ deg$). The wave motion is almost linear at the range of low frequency ($f/f_w=0.85$), and than becomes unsymmetrical about the still water level surface as the increasing of the wave amplitude. The higher harmonic waves, i.e., more than 2 peaks in one cycle of excitation can be observed. At $f/f_w=1.10$, the wave amplitude jumps down, and then the wave sloshing becomes linear. The other cases in Table 3.6 also demonstrate the same trend. These phenomena are similar to those in the experiment of TLD subjected to horizontal motion, and indicate that the nonlinearities of shallow liquid sloshing is strong.

4.3.2 Frequency Response

The experiment results of the frequency response of η'_{max} and η'_{min} as defined in Section 4.1 are shown in Fig. 4.6. The numerical simulations were also carried out corresponding to the experimental cases. In the computation, the TLD was excited from rest, and the computation continued until 120 periods of excitation, where the response of liquid motion was regarded to be steady state. The values of η'_{max} and η'_{min} are calculated by taking average value in last 20 cycles. The excitation frequency swept within the range of $0.8 \le f/f_s \le 1.2$ with a interval of 0.005.

From Fig. 4.6, it is found again that the nonlinearities of liquid sloshing are similar to those in TLD subjected to horizontal motion. The results of the case R6N1-01 (Fig. 4.6a) shows a good agreement between the experiment and simulation. However, for the cases R6N1-02 (Fig. 4.6b) and R6N1-03 (Fig. 4.6c), the simulation values are larger than the experimental ones. This may be due to the underestimated damping of liquid sloshing in the simulation. For the case of R6N1-04, the agreement around the resonance was not so satisfactory. This disagreement may due to that the experimental equipment could not generate purely sinusoidal motion as described in the sub-section 3.2.1. Several examples of time histories of the base displacement θ for the case R6N2-01 are shown in Fig. 4.7. It can be observed that the motion are not sinusoidal.

Figure 4.5 Experimental results and simulations of time histories of liquid surface elevation (Pitching motion, h=3.0cm, θo=0.1deg)

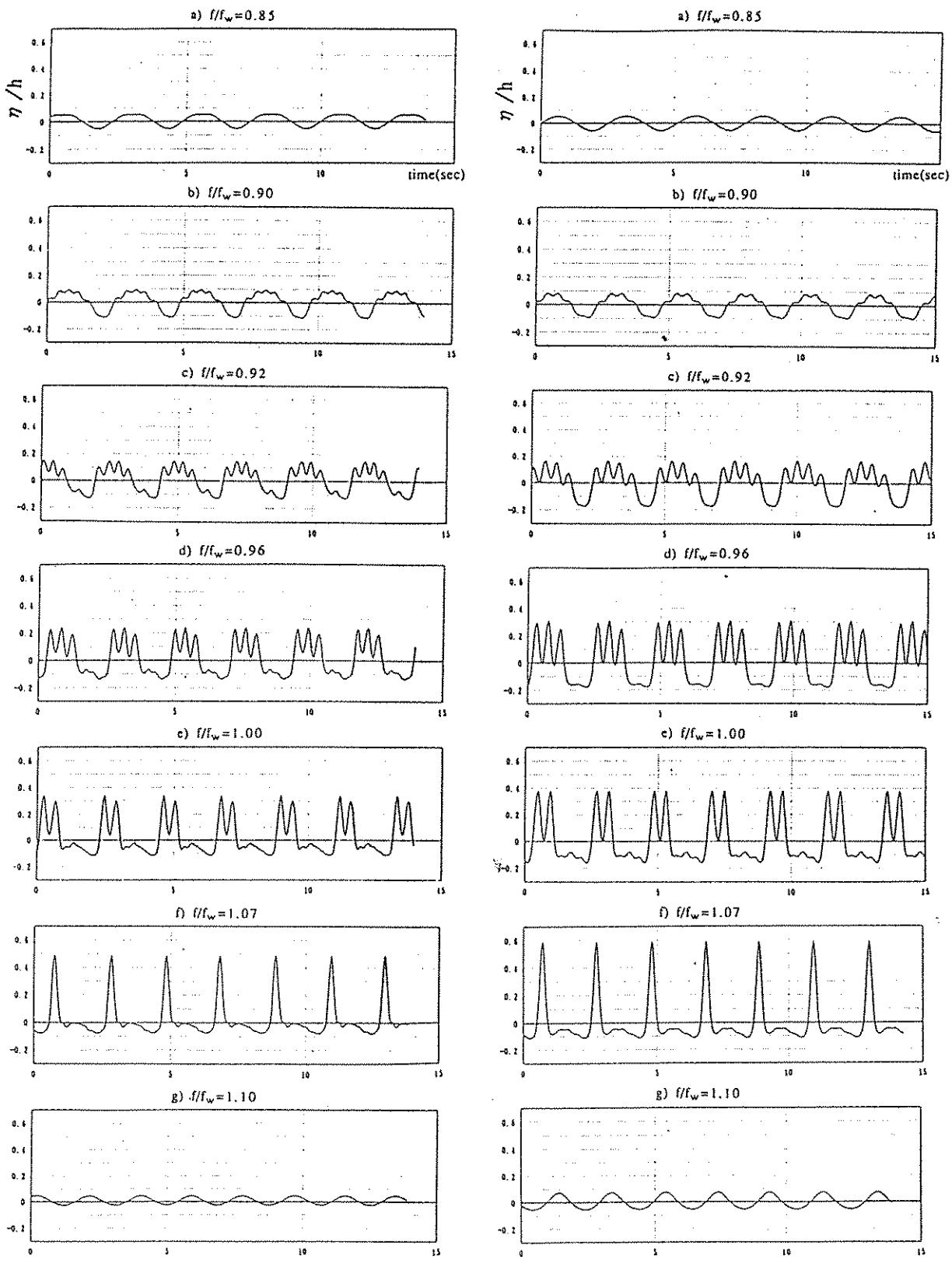

Figure 4.6 Frequency responses of liquid surface elevation (Pitching motion).

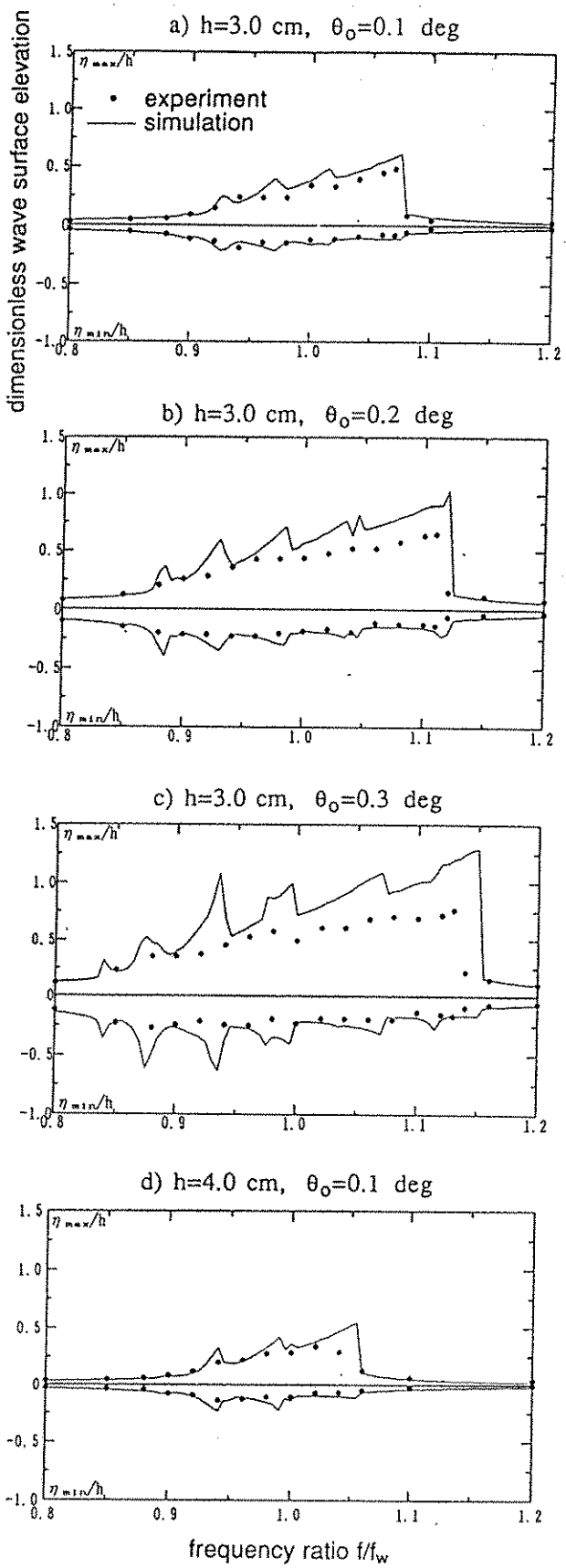

Figure 4.7 Examples of wave forms of excitation (for Case R6N2-01).

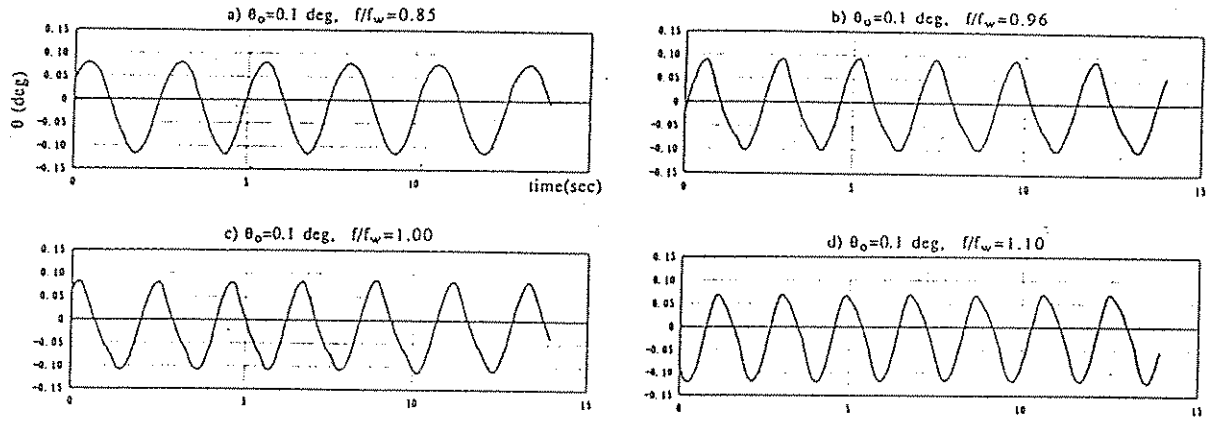

4.4 TLD-STRUCTURE INTERACTION

4.4.1 TLD-Structure Interaction Under Horizontal Motion

Both the experimental and simulation results of the responses of the structure with TLD are shown in Fig. 4.8. Note that the setting orientation of the tank relative to the direction of platform motion is different for the cases in Fig. 4.8a and Fig. 4.8b. It can be seen that the vibration amplitude is reduced drastically upon the installation of the TLD. No obvious breaking waves were visually observed in either case. Comparing Fig. 4.8a and 4.8b, however, it appears that the tank with $2a = 25\ cm$ and $h = 2.1\ cm$ has a better performance than that with $2a = 32\ cm$ and $h = 3.6\ cm$. This can be attributed to the difference in liquid damping of the two cases, as further discussed in the sub-section 5.2.2.

The results of the numerical simulation using the TLD model agree well with the experiment. Small discrepancies can be observed that may be partly due to some irregularities in the shape of the tank. A commercially available tank made of polypropylene has been used, although it is not perfectly rectangular, e.g., the bottom is not completely flat. Note that the numerical analysis is sensitive to the liquid depth h in terms of value and position of local peak in the frequency response. Small error in evaluation of h is not avoidable.

4.4.2 TLD-Structure Interaction Under Pitching Motion

The numerical simulations were carried out for TLD-structure interaction subjected to pitching motion to investigate TLD efficiency. In the case of horizontal motion, the total force of liquid sloshing acting on the vertical walls of TLD tank works as the suppressing force. In the case of pitching motion, the interaction force is the moment due to liquid sloshing inside TLD tank. This moment consists of not only the forces acting on the side walls of TLD but also the forces acting on the bottom of the tank as expressed by Eq. (2.71).

Figure 4.8 Frequency response: Numerical simulation and experiment

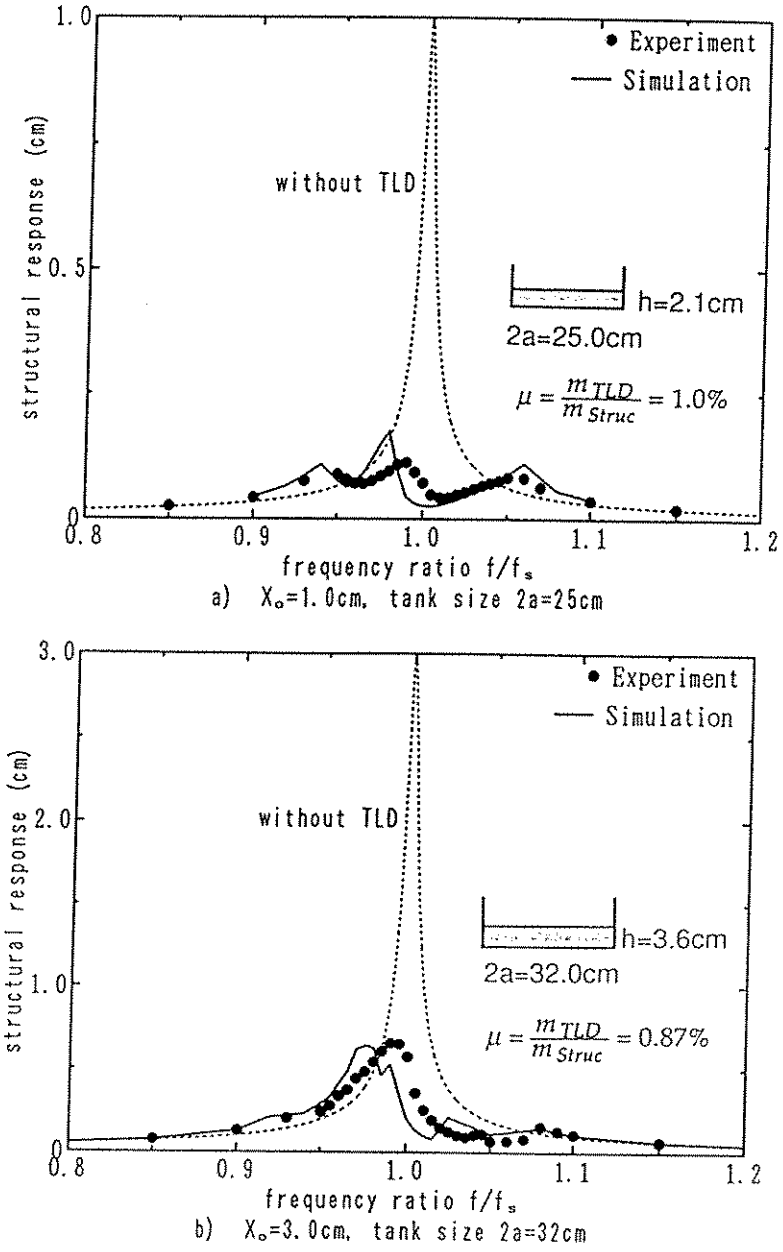

The external moment θ_e is assumed to be sinusoidal. The simultaneous equations (Eqs.(2.86), (2.66) and (2.67)) were solved by Runge-Kutta-Gill method with time step $\Delta t = 1/60$ of the excitation period. The computing was executed until 120 cycles, where it is regarded that the motions of both structure and liquid in TLD are at steady state. The size of TLD tank is: $2a = 59\ cm$, $b = 16.75\ cm$, and water depth $h = 3.0\ cm$. The damping ratio of structure, ξ_s is about 0.24%, and the natural frequency, f_s, is 0.458 Hz. The results are shown in Fig. 4.9, I_w is the moment of inertia of liquid in TLD around the origin O (Fig. 2.10) when the liquid inside is at rest state.

As shown in Fig. 4.9, the efficiency of TLD for pitching motion is satisfactory. Because the suppressing moment due to the shift of weight center of liquid is much lager than that due to horizontal sloshing force, it is found that TLD can suppress pitching motion even the moment ratio I_w/I_s is as small as 0.001%. An experiment should be carried out to verify the numerical simulations in the future study.

Figure 4.9 TLD for suppressing pitching motion.

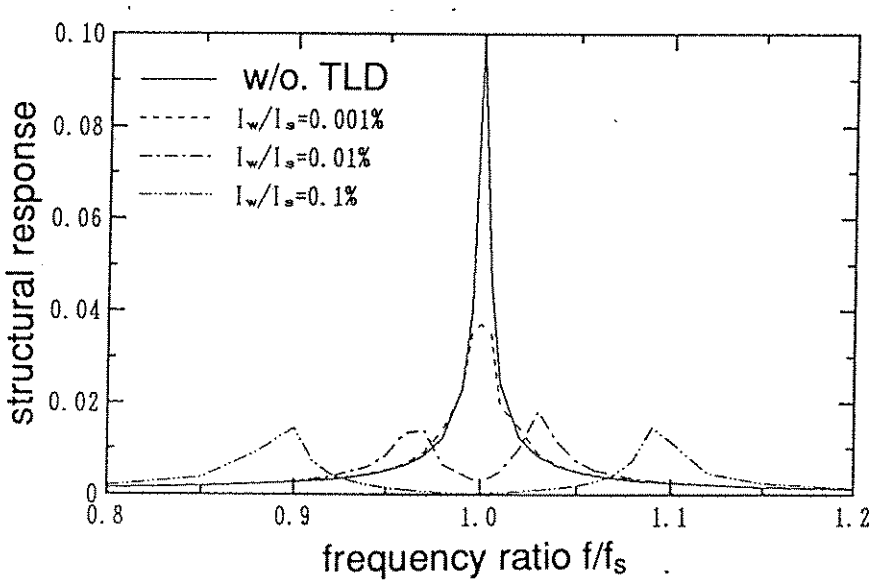

4.5 SOLA-VOF METHOD

4.5.1 TLD Under Small Amplitude Excitation

In the SOLA-VOF code, the basic equations are Navier-Stokes equations, and the no-slip boundary conditions were used. The equations were solved directly by the difference method. The special treatment was included for free surface so that the method used is expected to be valid for breaking wave situation. Due to the equations were directly solved, the effect of liquid viscosity was taken into account naturally. Therefore the approach was also valid for high viscosity liquid sloshing. The dispersion relation is included implicitly so it is no need to be treated in SOLA-VOF code unlike in the TLD model proposed previously.

The example computed is illustrated in Fig. 4.10. The TLD tank is *59.0cm* in length and *10.0cm* in height, filled with *3.0cm* water. The meshes for numerical computation distribute in the area of *59.0cm* x *10.0cm* as shown in Fig. 4.10. m and n denote the mashes numbers in length direction and height direction, respectively. The base excitation is sinusoidal and is with an amplitude of $A=0.1\ cm$.

The accuracy of computation is affected by the number of mesh. The computation with large number of mesh gives accurate results but takes more

Figure 4.10 A example solved by using SOLA-VOF Code.

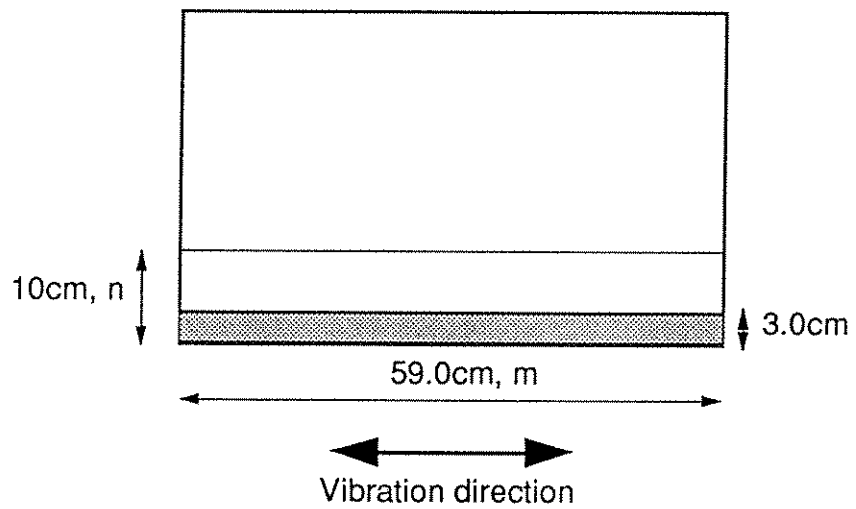

Figure 4.11 Experimental and simulation results.

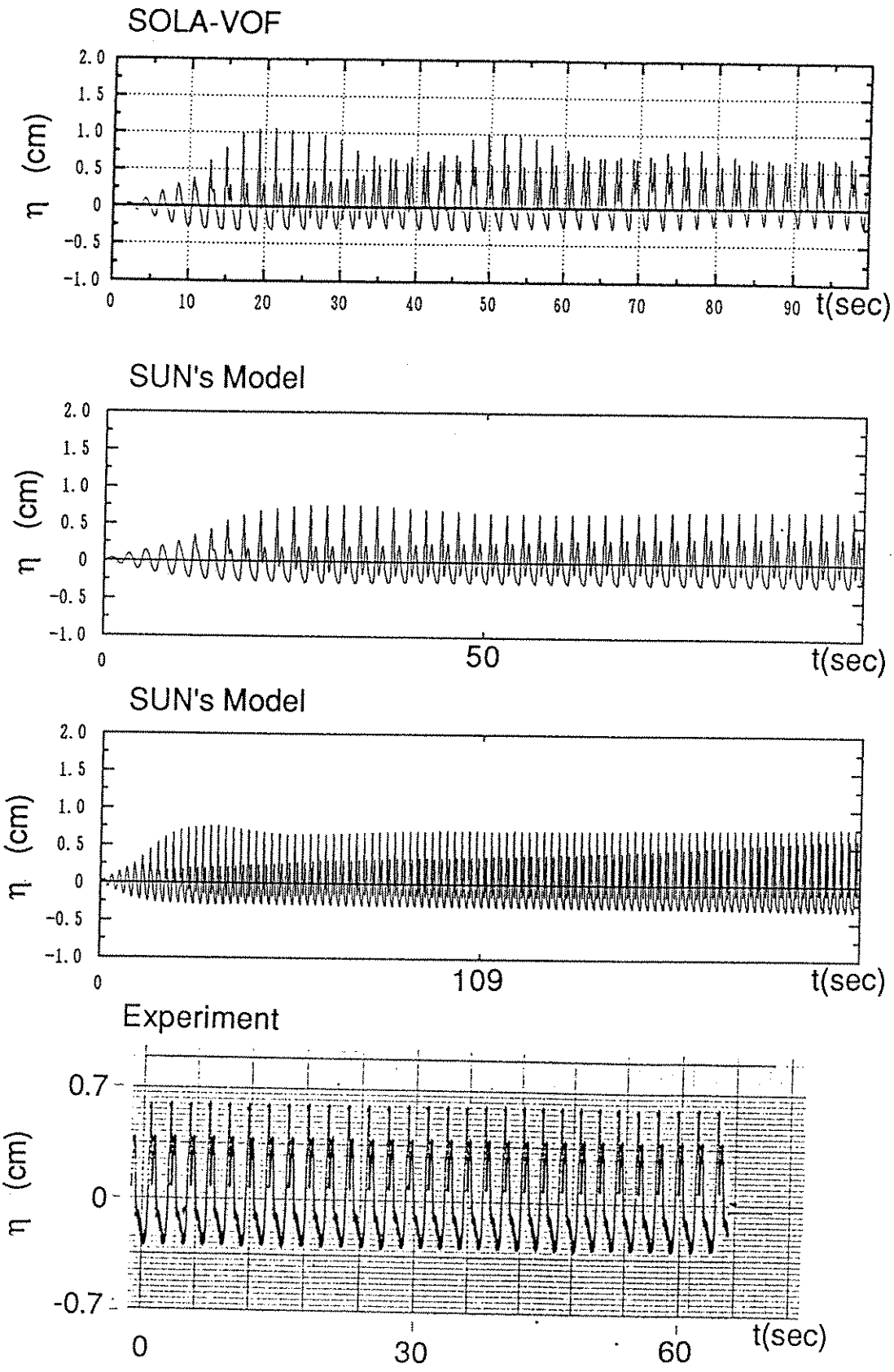

CPU time. The test computations have been done in order to determine the mesh numbers m and n for the problem described above. Increasing the mesh number, mxn from $10x10$ to $20x20$, the wave elevation time histories changed a lot. However, when the number of mesh was increased from $30x30$ to $40x40$, the time histories did not change so much, but the time consuming increased terribly. It is difficult to conclude a general relation between the accuracy and the mesh numbers. The test example can be $30x30$, with which the accuracy of computation is satisfied and the time consuming is also acceptable. The computations by SOLA-VOF discussed in this chapter were carried out by employing the mesh number $30x30$. The liquid in TLD is rest initially and the computation lasted until 100 excitation cycles. The excitation frequency ratio f/f_w is 1.00. The length of time step of computation is adjustable automatically in the SOLA-VOF code.

The simulation results computed by SOLA-VOF are shown in Fig. 4.11. For comparisons, the simulation results from the proposed TLD model and the experimental results are presented also. It is found that the liquid sloshing is strongly affected by second harmonic component at the excitation frequency ratio of 1.00. Two peaks can be observed in one excitation cycle from both the simulations by SOLA-VOF or the proposed model and the experiment. It is found that the SOLA-VOF also can simulated the higher harmonic effect on liquid sloshing even though the wave forms between the simulation results and the experimental ones is slightly different.

4.5.2 TLD Under Large Amplitude Excitation

The computation was carried out by using SOLA-VOF code for the case with a excitation amplitude $A=1.0\ cm$, under which the wave sloshing is broken as known from the experiment. The mesh number was $30x30$ and the time of excitation was $20sec$, it took the CPU time $30\ min$ by using the mainframe of the University of Tokyo (HITAC M680).

The results are shown in Fig. 4.12. The wave form is triangular like, which indicates that breaking waves occurred as observed from the experiment. However, the center line of wave surface elevation goes up as the increasing of computing time and the wave surface becomes always positive when the excitation time is over 20sec. This is not reasonable in practice. Compared with the experiment results (Fig. 4.13), the wave form is similar in first several cycles

Figure 4.12 Simulation results for liquid sloshing with breaking waves.

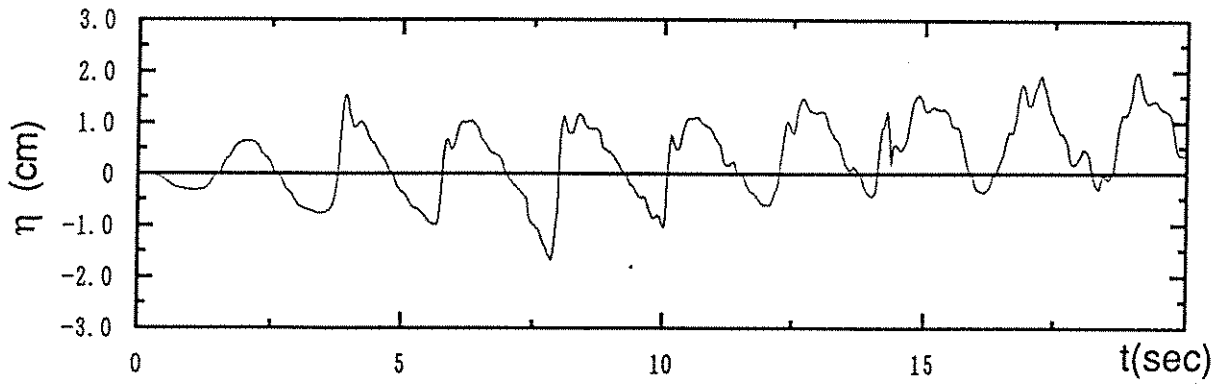

Figure 4.13 Experimental results for liquid sloshing with breaking waves.

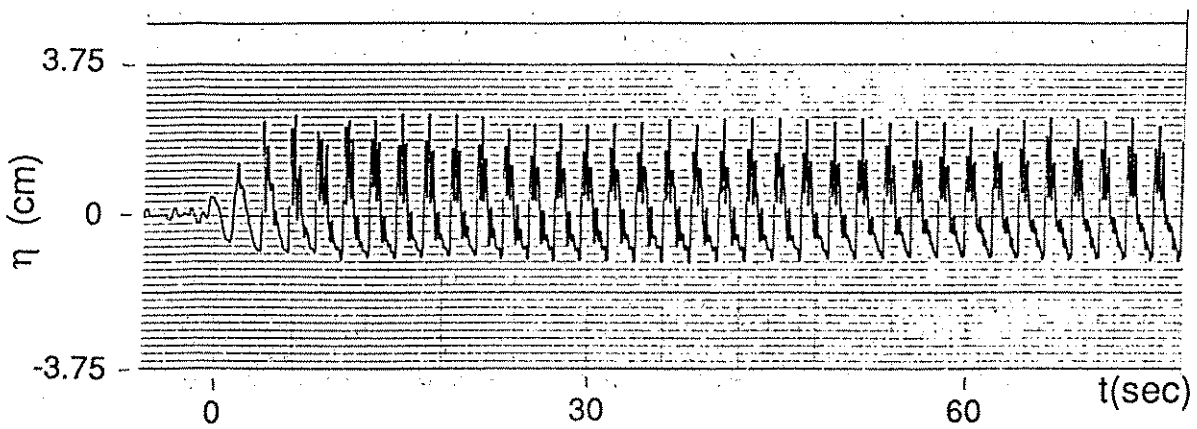

and then becomes quite different. The results by SOLA-VOF are not agree with the experimental one. This method may have problems for computing liquid sloshing with wave breaking.

The computation time consuming increases enormously, as compared with the simulation case when the excitation amplitude, A is $0.1cm$. This can be explained as that the time step has been adjusted automatically to be very small when the velocities of liquid particles increase under a large base amplitude

excitation, since an automatic time-step control is included in the SOLA-VOF code. In the computation, after several cycles of excitation, it is found that the increase of pressures in the free surface cells are vary large even the time step is small. This is considered to lead to a large computational error.

It seems difficult to treat the problem of liquid sloshing with wave breaking by using numerical simulation means at present. Even a number of method, for example, MAC, SOLA-VOF, etc., have been developed, there are still some problems on the treatment of boundary condition, free surface condition, viscosity and even the approach of simulation.In order to have better quantitative agreement, a lot of effort must be devoted for the improvement of the present method.

However, SOLA-VOF code may be used to demonstrated the mechanism of damping of liquid motion due to wave breaking and submerged blocks, which is just for scientific purpose.

CHAPTER 5 MECHANISM AND DAMPING CONTROL OF TLD

5.1 PROPERTIES OF TLD

For designing a TLD, the basic parameters, such as the natural frequency or the damping of liquid sloshing should be investigated and discussed. These parameters are affected by TLD tank size, liquid depth, liquid velocity etc.. Moreover, they are also dependent upon the wave amplitude or the excitation amplitude of the base since the liquid sloshing in TLD is nonlinear. To design a required TLD, it is necessary to choose suitable tank size, liquid depth and liquid viscosity for suppressing structural vibrations. Therefore, the relationships between these physical quantities (tank size, etc.) and TLD properties souled be made clear.

5.1.1 Nonlinearities

Hardening System And Softening System. The natural frequency of liquid sloshing in TLD depends on the base excitation amplitude. As shown by the experimental results discussed in Section 4.2, the nonlinearity of shallow liquid is hardening-type namely, the natural frequency of liquid becomes higher when the excitation amplitude increases. These property however could be changed with the depth ratio of liquid.

The experiments using various liquid depth ratios have been carried out and it is found that the liquid depth ratio, ε do affect the nonlinear type of the liquid sloshing. The experimental cases are shown in Section 3.1 (Table 3.3). The liquid sloshing is strongly hardening-type when the liquid is rather shallow with a depth ratio $\varepsilon=0.2$ (Fig. 5.1). The nonlinearity becomes weak as the depth ratio increases. When the liquid depth ratio $\varepsilon=0.6$, the liquid sloshing becomes almost linear; the frequency of liquid sloshing does not depend on the excitation amplitude and the peak of liquid surface elevation response curve locates at the frequency ratio of *1.00*, indicating that the natural frequency of liquid sloshing from the experiment agrees with that calculated from the linear theory. The frequency responses of the experiment results with the liquid depth ratio $\varepsilon>0.6$

show that the liquid sloshing becomes softening-type, namely, the frequency response curve bends to low frequency side.

Figure 5.1 Experimental result show nonlinearities of TLD.

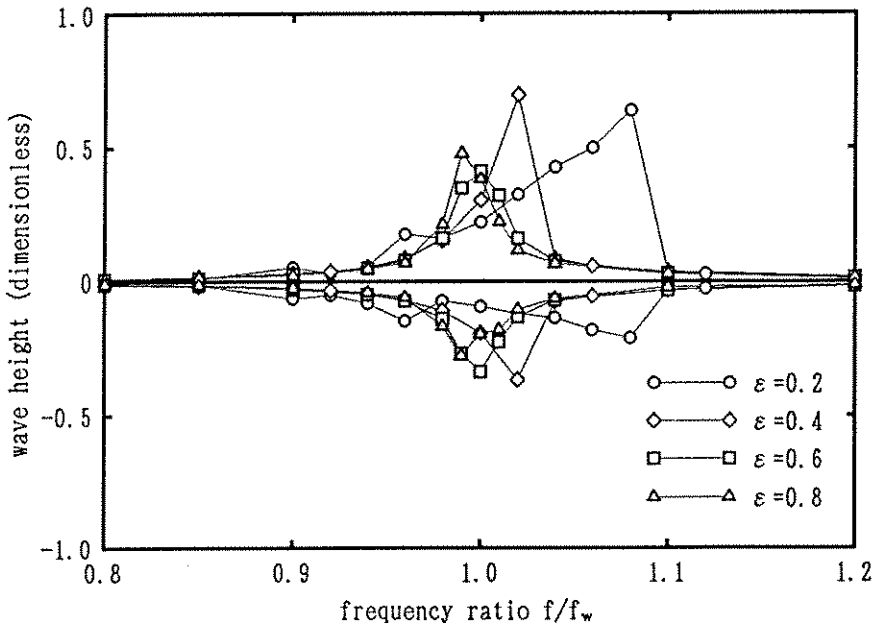

Figure 5.2 Hayama's simulation results.

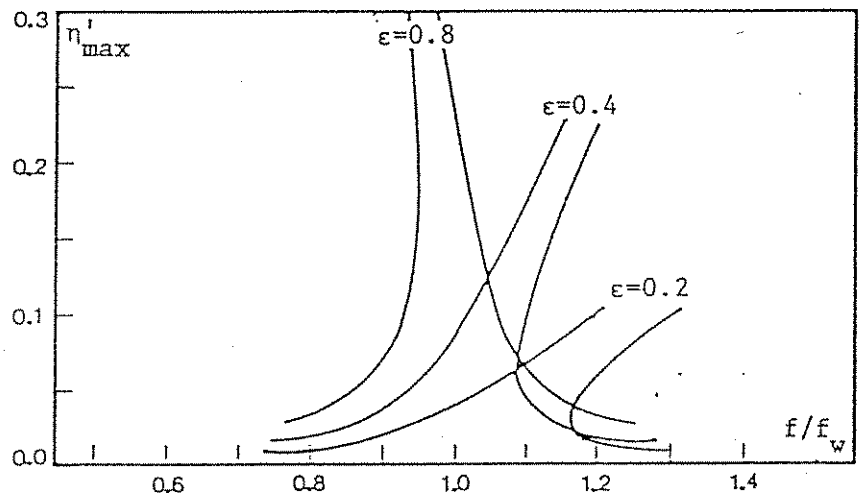

The Hayama's simulation [1987] also showed a similar trend. According to his simulation, the critical value of depth ratio classifying the system to hardening or softening is about *0.67* (Fig. 5.2). When the depth ratio $\varepsilon<0.67$ (liquid is shallow), the liquid motion is hardening, then it becomes to softening as the depth ratio $\varepsilon>0.67$. The liquid motion is linear when the depth ratio $\varepsilon= 0.67$.

In Bauer's paper [1969], he also mentioned this property of liquid sloshing in a rectangular tank. However, the model proposed by him predicted the critical value of liquid depth ratio is *0.41*, which is different from either the experimental results or the simulation by Hayama.

Higher Harmonics. From the shaking table experiments, the local peaks of the wave surface elevation response curve can be observed at the excitation frequency range lower than the jump-down frequency. The higher frequency components which approximately have integer times of the fundamental frequency of liquid sloshing can be observed from the time history corresponding to the local peaks in the frequency response curves. These are the effects of higher harmonics of liquid sloshing.

The presence of higher harmonics of liquid sloshing in TLD are due to superharmonic resonance of higher modes of liquid sloshing. Since the motion of TLD tank is horizontal, only the unsymmetrical modes of liquid sloshing are excited. For liquid sloshing in a rectangular tank, the natural frequencies of each unsymmetrical modes are

$$\omega_n = \sqrt{\frac{2n-1}{2a}\pi g \tanh\left(\frac{2n-1}{2a}\pi h\right)} \qquad (n=1,2,\ldots) \tag{5.1}$$

For shallow liquid sloshing, the above equation can be simplified as

$$\omega_n \approx \frac{2n-1}{2a}\pi\sqrt{g\,h} \qquad (n=1,2,\ldots) \tag{5.2}$$

Therefore, the ratio between any two natural frequencies of unsymmetrical sloshing modes are

$$\omega_i : \omega_j \approx (2i\text{-}1) : (2j\text{-}1). \tag{5.3}$$

From this, the relations between the natural frequencies of unsymmetrical sloshing modes are

$$\omega_1 : \omega_2 : \omega_3 : \ldots \approx 1 : 3 : 5 : \ldots . \tag{5.4}$$

From the Eq. (5.1), for example, the natural frequencies of a TLD with $2a = 59.0\ cm, h = 3.0\ cm$, have the relation expressed as

$$\begin{aligned} \omega_1 : \omega_2 : \omega_3 &= 2.876 : 8.357 : 13.162 \\ &\approx 1 : 2.9 : 4.6 . \end{aligned} \tag{5.5}$$

This can be also written in the form of

$$\omega_1 : \frac{1}{3}\omega_2 : \frac{1}{5}\omega_3 \approx 1.0 : 0.97 : 0.92 . \tag{5.6}$$

The superharmonic resonance phenomena will occur near the primary resonance; i.e., the second unsymmetrical mode presents at the frequency of

Figure 5.3 Experimental results show higher harmonic effects.

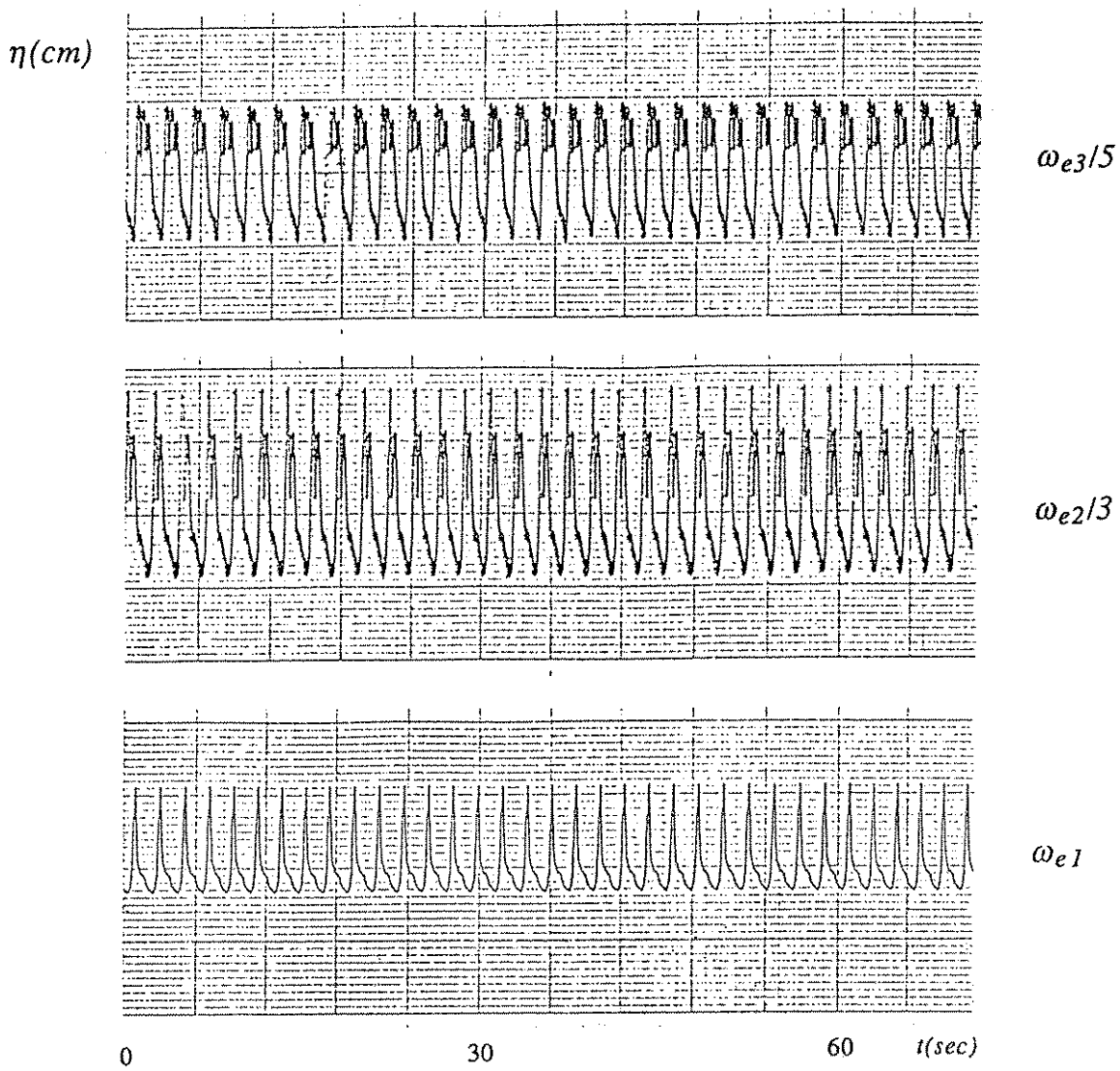

$\omega_2/3 \approx 0.97\omega_1$, which is slightly less than ω_1, and the third mode does so at the frequency of $\omega_3/5 \approx \omega_1$.

Figure 5.3 shows the time histories of experimental results (Case 6N1-01, table 3.1) for the wave surface elevation. The cubic nonlinearity of 2nd mode of liquid sloshing and other higher harmonics nonlinearity (e.g., 3rd mode) can be observed. Corresponding to these three time history curves, the frequencies are $\omega_{e1}=3.035$ Hz,, $\omega_{e2}=2.884$ Hz, and $\omega_{e3}=2.771$ Hz, respectively., where ω_{ei} is the natural frequency of i^{th} mode of liquid sloshing observed from the experiment. The ratios of them are

$$\omega_{e1} : \omega_{e2} : \omega_{e3} \approx 1.0 : 0.95 : 0.91 . \tag{5.7}$$

This ratio is quite close to that expressed in Eq. (5.6). One can see that the linear natural frequency equation (Eq. (5.1)) can be used to predict approximately the relation between the higher harmonic modes even the natural frequencies themselves shifted toward high frequency side due to the hardening-type nonlinearity as observed from the experiments.

The superharmonics of higher modes with the natural frequencies which are the odd times of the fundamental natural one are only induced, because the liquid is sloshing under a horizontal excitation. The effects of higher harmonics are more significant when the liquid is shallower. As the liquid becomes deep, the higher modes frequencies will no longer be a integer times of the fundamental one, and as a result, the superharmonic effects become weak.

The superharmonic nonlinearity of liquid sloshing make the frequency response more complicated. The local peaks due to these higher harmonic effects also can be observed from the structure response curve of TLD-structuer interaction example (Fig. 4.8a).

5.1.2 Natural Frequency

The linear undamped natural frequency of liquid sloshing can be calculated theoretically by the formula

$$f_w = \frac{1}{2\pi}\sqrt{\frac{\pi g}{2a}\tanh\left(\frac{\pi h}{2a}\right)} . \tag{5.8}$$

This is obtained only when wave amplitudes of liquid sloshing are small and the liquid motions are regarded as linear.

Figure 5.4a Effect of tank size on natural frequency.

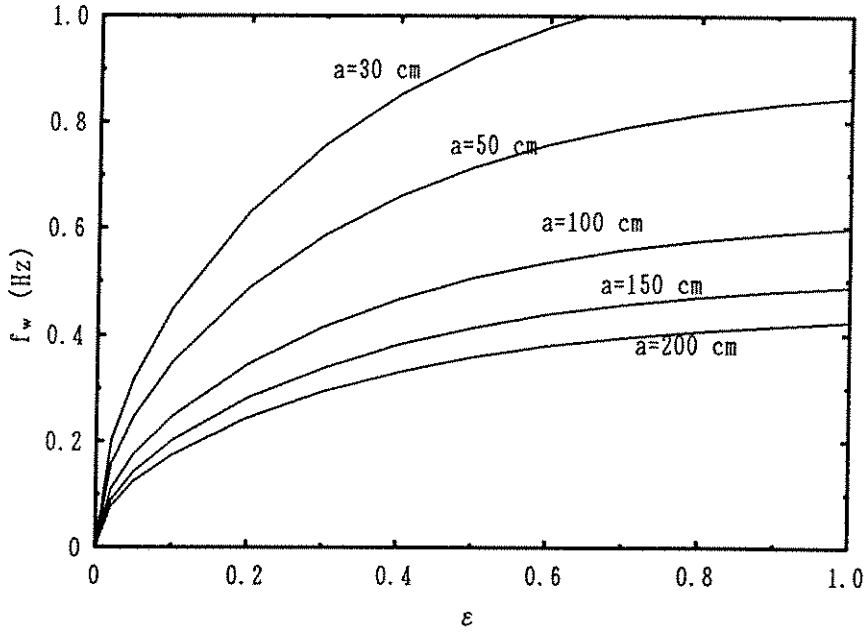

Figure 5.4b Effect of liquid depth ratio on natural frequency.

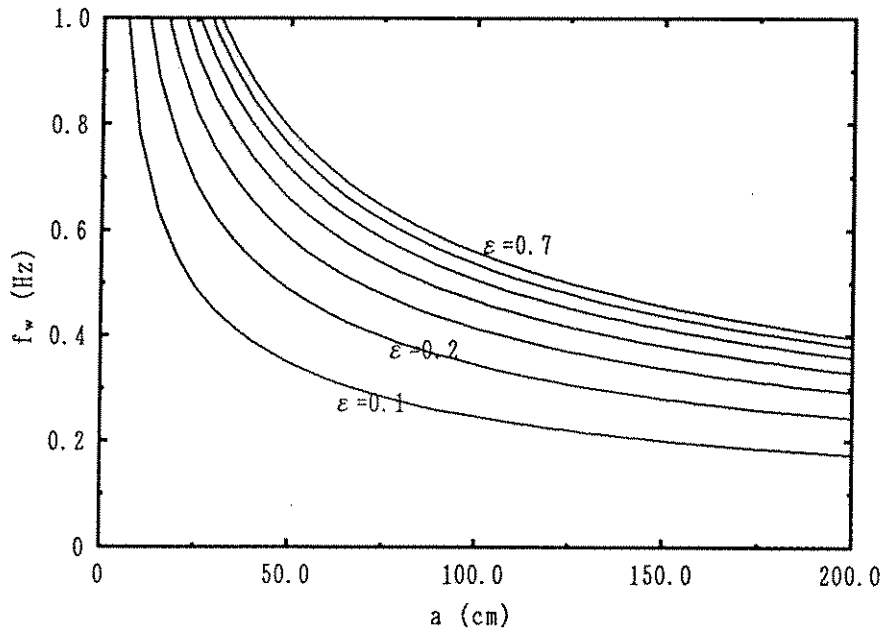

Figure 5.4c Relation between tank size and liquid depth ratio for a given frequency.

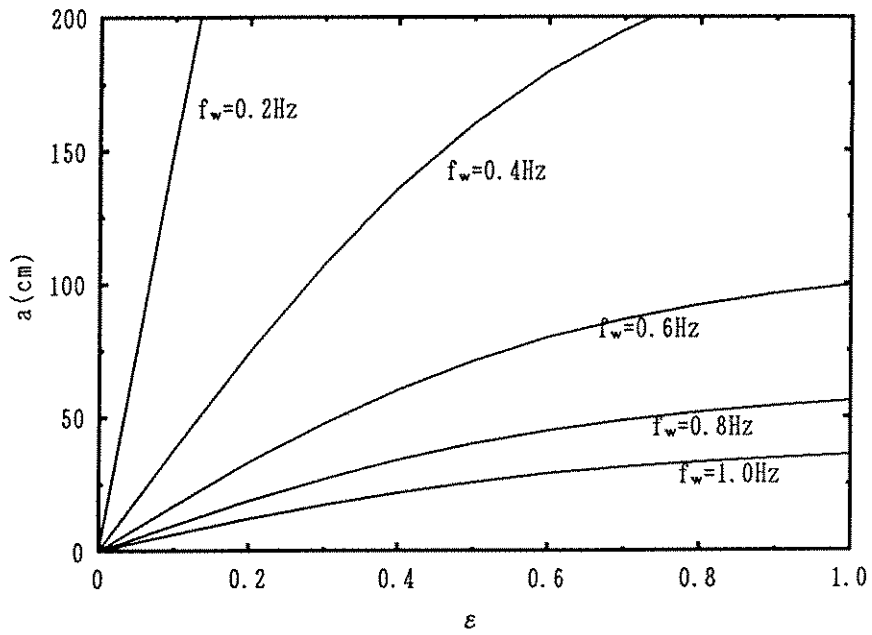

The effect of damping on the natural frequency is negligible if water is used as the liquid in TLD since it gives very low damping. For liquid sloshing with large wave amplitude, the resonant frequency shifts away from the natural frequency calculated by Eq. (5.8) due to the nonlinearity of liquid sloshing. As discussed in sub-section 5.1.1, the frequency-response curve of surface elevation bends toward high frequency side or low frequency side due to nonlinearity of liquid sloshing corresponding to that the liquid depth ratio is small *(<0.6)* or large *(>0.6)*.

The natural frequency of liquid sloshing depends on the wave amplitude. It is impossible to tune a TLD perfectly to the structure at any excitation amplitude. The natural frequency of TLD deviates from the linear (Eq. (5.8)) with a relative error of *10-15%*. When designing a TLD, Eq.(5.8) is usually used, It should be noted that this may lead to that the TLD designed mis-tunes to the target structure.

Equation (5.8) shows that the linear natural frequency is dependent upon the TLD tank size a and the liquid depth ratio ε. Figure 5.4 shows the relation among f_w, a, and ε. The following discussions are carried out in the ranges of $f_w<1.0$Hz, $a<200cm$, and $\varepsilon<1.0$.

For a TLD with a given depth ratio e, the natural frequency f_w decreases as the TLD tank size a becomes large. The natural frequency is more significantly affected by the tank size when TLD tank is small (e.g., $a<50cm$), while is not sensitive when TLD tank is large (e.g., $a>150cm$) (Fig. 5.4a). In a depth ratio range, the frequency f_w can vary largely for a smaller size TLD tank (Fig. 5.4b).

Large liquid depth ratio ε results in a high natural frequency f_w for a TLD with a given tank size a (Fig. 5.4b). The natural frequency f_w is more sensitive to ε for a small value (e.g., $\varepsilon<0.2$). Generally, the natural frequency f_w is significantly affected when tank size a and liquid depth ratio ε are small.

Figure 5.4c suggests that to design a TLD with low natural frequency (e.g., $f_w=0.2Hz$), the liquid depth ratio ε should not be too large, to avoid an extremely large size tank. On the other hand, a very small tank size should be used to make liquid shallow when design a TLD with high natural frequency (e.g., $f_w=1.0Hz$).

5.1.3 Damping of Liquid Sloshing

Damping of liquid sloshing in TLD significantly affects its effectiveness as a damper and is an important parameter in design as will be discussed in Section 5.2. Using only plain water leads to a very low liquid damping. The structure with a low-damping TLD has large responses at certain excitation frequency. The details will be discussed in next section. When the optimal liquid damping in TLD, the vibration of the structure can be suppressed in a wide range of frequency.

For TLD with plain water, the damping of liquid sloshing is due to the friction in the boundary layers and the surface contamination on the free surface. In the model proposed in Section 3.2, the damping of liquid sloshing was semi-analytically treated to be linearly proportional to the velocity of liquid particle u (Section 2.3). A damping coefficient λ is introduced as expressed by Eq. (2.46).

The damping coefficient λ is affected by the tank size a and the liquid depth ratio ε. For a simple understanding, the damping ratio ξ_w of liquid sloshing based on the linear wave theory (Appendix D) is expressed as

$$\xi_w = \frac{\lambda}{2\omega_w}, \tag{5.9}$$

i.e.,

$$\xi_w = \frac{1}{\eta+h}\frac{\sqrt{2}}{2}\frac{\sqrt{\omega\nu}}{2\omega_w}(1+2h/b+S)\,. \tag{5.10}$$

Assuming that the wave amplitude is small, i. e., $\eta << h$, and the TLD tank configuration has $2h/b=20\%$, and the surface contamination factor takes the value of 1.0. The damping ratio can be expressed as

$$\xi_w = \frac{1}{a\varepsilon}\frac{\sqrt{2}}{2}\frac{1}{2}\sqrt{\frac{\nu}{\omega_w}}\,(1.0+0.2+1.0)\,, \tag{5.11}$$

where the liquid used is assumed to be water, so $\nu=0.01\ cm^2/s$. For a TLD with $2a=59.0cm$, $h=3.0cm$, the relation expressed by Eq.(5.11) is shown in Fig. 5.5. The damping ratio ξ_w decreases as the liquid depth ratio ε or the tank size a increases. As shown in Fig. 5.5, the damping ratios becomes very small, easily less then 1.0% when the liquid depth ratio ε is larger than 0.2. These damping values are much smaller than the optimal value 6.0% as discussed in Section 5.2. For the liquid depth ratio $\varepsilon<0.1$, the damping ratio increase sharply as the liquid depth ratio ε decreases. This suggests that the shallow liquid (small liquid depth ratio) should be used to obtain higher damping of liquid sloshing close to the optimal damping value.

From the experiment, we found that the damping of liquid sloshing is not linear viscous damping. It depends upon the excitation frequency and the wave amplitude. The liquid damping was investigated experimentally and was

Figure 5.5 Relation between damping ratio and liquid depth ratio.

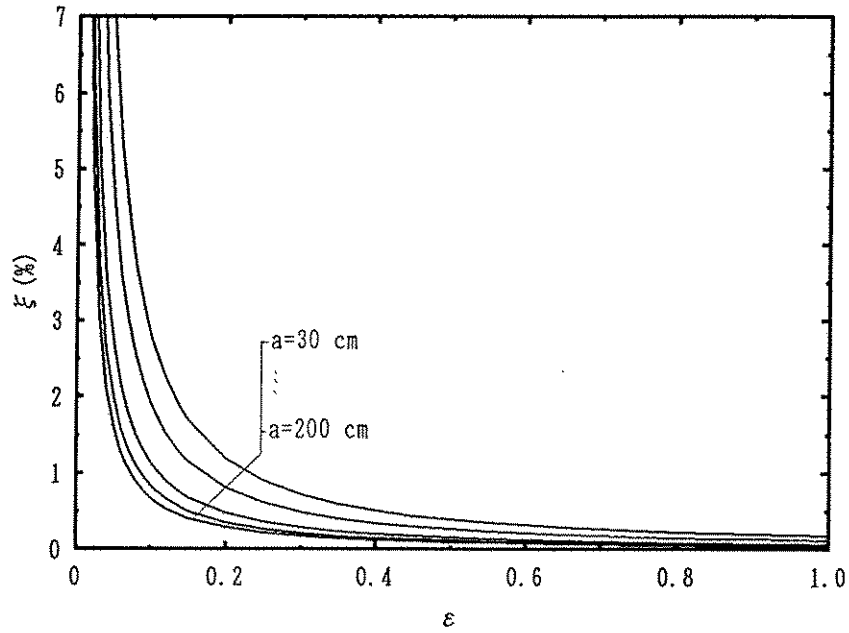

quantified by using TLD Analog [Fujino at. el. 1990]. Generally, the damping of liquid sloshing increases as the excitation amplitude increases. For the liquid sloshing with breaking waves under a large excitation amplitude, the energy dissipation due to breaking waves is another source of damping of liquid sloshing. It is necessary to increase the damping of liquid sloshing to make TLD more effective. The means to increase the damping will be discussed in Section 5.3.

5.2 MECHANISM OF TLD AND COMPARISON WITH TMD

The understanding of the mechanism of TLD is necessary to use TLD as a damper. The mechanism of TLD is regarded to be similar to that of TMD, which is a well-known mechanical damper. In this section, the mechanism of linear TMD is explained using the concept of energy shutter. On the basis of understanding TMD, the mechanism of TLD is explicated. The optimization and the effectiveness of TLD as compared with TLD are discussed.

5.2.1 Mechanisms of TMD and TLD

TMD is a kind of well-known mechanical damper. Considering a system of SDOF structure and a linear TMD (Fig. 5.6), the mechanism of TMD can be explained by the energy concept. TMD damps the structural vibration through two ways: one is to shut out the part of the energy input from outside; and another is to dissipate the energy inside the system (SDOF structure + TMD).

The structure without TMD has a large vibration amplitude at the resonance because it absorbs the most energy from outside at this frequency. After attaching TMD to the SDOF structure, the whole system can be treated as a 2DOF one. The dynamic characteristics of the structure are changed. The energy input from outside to the system are calculated both for the structure with a optimized TMD and for that without TMD (Fig. 5.7). It is found that TMD works like a energy shutter so that the energy input to the structure near the resonance can be shutted out. TMD also dissipates the vibrational energy of the structure owing to its damping.

Figure 5.6 Tuned mass damper.

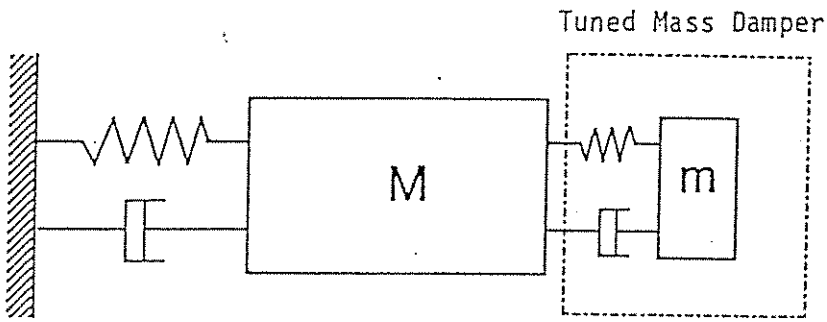

Figure 5.7 Energy input per cycle into the structure.

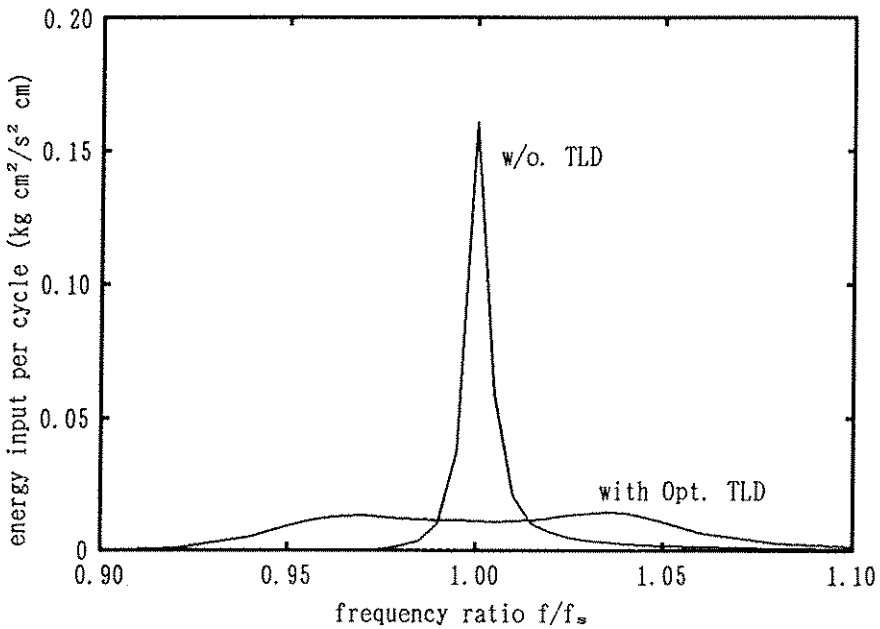

The mechanism of TLD is basically similar to that of TMD [Fujino et. al. 1990]. As a damper, TLD is attached to a structure in order to change the dynamic characteristics and to dissipate the vibrational energy of the structure. The liquid in TLD can be simply regarded as a SDOF system like TMD when the excitation

frequency is near the first resonance and the wave amplitude of liquid sloshing is small. The performance of TLD, however, will become nonlinear when the wave amplitude is large, namely, it nonlinearly depends both on the excitation amplitude and on the excitation frequency. The vibrations of structure attached with TLD are suppressed also by shutting out the input energy and dissipating the vibrational energy of the structure due to liquid sloshing in TLD. Because of the effects of nonlinear stiffness, higher harmonics, and nonlinear damping of liquid sloshing, the performances of TLD is more complicated as compared with TMD.

5.2.2 Optimal Parameters for TLD Design

The maximum responses of the structure can be reduced if a TMD is optimized. Similar to TMD, the mass ratio, frequency ratio and damping of liquid sloshing are the parameters to be controlled in the design of TLDs. Usually, the ratio of the liquid mass to the structural mass is around *1%*; and the fundamental natural frequency, f_w of liquid sloshing (Eq. 2.26) is designed to tune the natural frequency of structure, f_s, i.e., $f_w/f_s \approx 1.00$.

For given mass ratio μ and frequency ratio, an optimal damping value exists for TLD to give good performance. Warburton and Ayorinde [1980] suggested that the optimal damping ratio for TMD (μ=1%) is *6.0%* for harmonic excitation.

Figure 5.8 Effect of liquid damping on TLD performance.

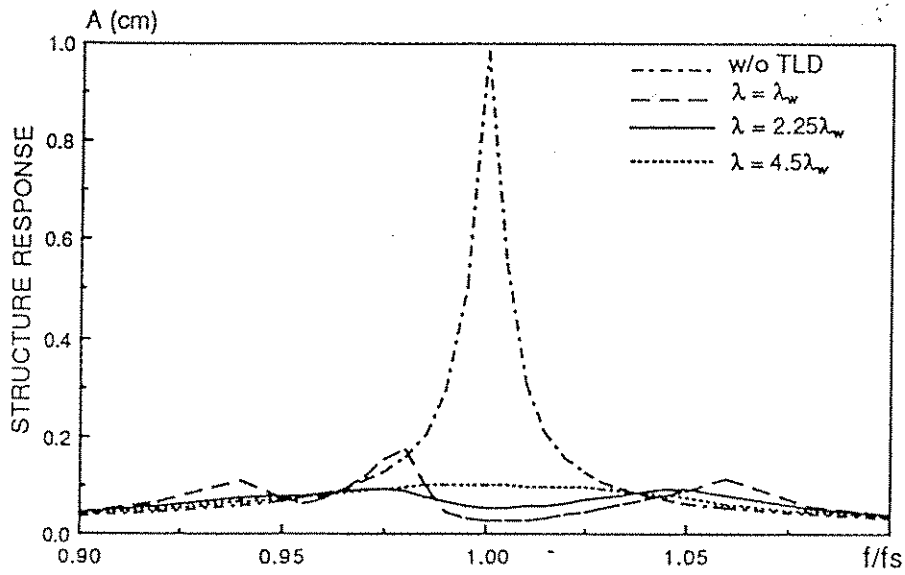

Figure 5.8 shows simulation results on the effect of the damping of liquid motion on TLD-structure interaction ($m = 1\%$, $f_S = 0.91$ Hz, $2a = 25$ cm, $h = 2.1$ cm and $\xi_S = 0.32\%$). The structural response curves for various liquid damping of TLD ($\lambda = \lambda_w$ (plain water), $2.25\lambda_w$, and $4.5\lambda_w$) are plotted in the figure. It appears that, when the liquid damping is $2.25\lambda_w$, the structural response becomes almost flat over the frequency range considered, and is suppressed effectively. Indeed the liquid with appropriately high damping significantly improves the efficiency of TLD. the means to control damping of liquid sloshing will be discussed in the next section.

5.2.3 Effectiveness of TLD Compared with TMD

Figure 5.9 shows the frequency response curves for comparing TLD and TMD effectiveness. Both dampers are optimized with a selected mass ratio of 1%. The optimal parameters of TMD are determined according to Warburton and Ayorinde's paper [1980]. TLD tank in this example is the same as that used in the preceding example, and $\lambda = 2.25\lambda_w$ is optimal in this case. It is found in Fig. 5.9 that, if optimized, the efficiency of TLD is almost equal to that of TMD.

Figure 5.9 Comparison of TLD and TMD when optimized.

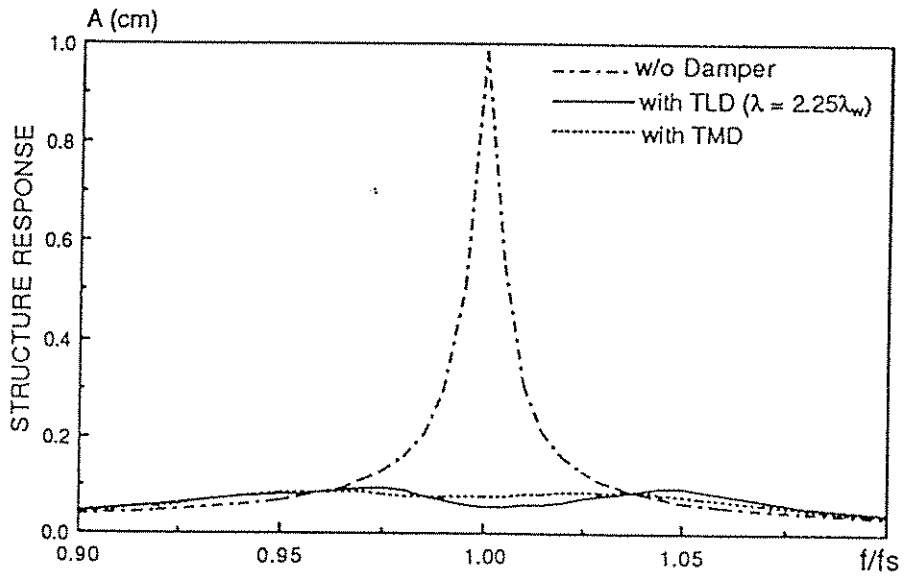

5.3 CONTROL AND EVALUATION OF DAMPING OF LIQUID SLOSHING

Among the basic parameters of TLD, the damping of liquid sloshing significantly affects the TLD efficiency. As discussed in the previous section, the optimal value of damping of TLD exists. Generally, the damping of liquid sloshing is less than the optimal value if plain water is used as liquid. Several means are investigated to increase damping of liquid sloshing, such as using shallow liquid, high viscosity liquid, or adding floating surface materials. The results are demonstrated and discussed in this section.

5.3.1 Damping of Liquid Sloshing in Shallow Water

Equation (5.11) shows that the damping ratio of liquid sloshing ξ_w is approximately inversely proportional to the liquid depth ratio ε for a given tank size of TLD. The high damping can be obtained by using shallow liquid (i.e., small liquid depth ratio). For example, from Fig. 5.5 we can know that TLD with the tank size of $a=30cm$ and the liquid depth ratio of $\varepsilon=0.06$ has a damping ratio of liquid sloshing, about 6%, which is regarded as the optimal value of TLD damping.

It was also found from the experimental results that the TLD with smaller liquid depth ratio has better effectiveness. The results in Fig. 4.8a has indicated that for around same mass ratio ($\mu = 1\%$) the tank with $2a = 25\ cm$ (and shallower h) was more efficient as a damper, than that with $2a = 32\ cm$. This can be attributed to the differences in damping of liquid motion. The liquid depth ratios for the tanks with $2a=25cm$ and $2a=32cm$ are 0.17 and 0.23, respectively. The damping of liquid sloshing with smaller liquid depth ratio is higher and is more closer to the optimal damping value.

Shallow liquid leading to higher liquid damping may therefore be expected to give better performance as a damper. However, it should be noted that the smaller size TLD's have to be used with shallow liquid to get certain natural frequency, inherently leads to larger number of TLD's to attain the same mass ratio. That may cause problems in the cost of the TLD tanks and the space required for TLD installation. On the other hand, waves in such a shallow-water TLD easily break in relatively small base-motion. The damping due to breaking waves is difficult to treat theoretically. The model proposed by the author is modified to account for the breaking waves. This will be discussed in Section 5.4.

5.3.2 Damping of Liquid Sloshing in High Viscosity Liquid

Instead of changing the TLD tank size and the liquid depth, the liquid damping can also be controlled by changing the liquid viscosity ν (Eq. 5.11).

The shaking table experiment using TLD with high-viscosity liquid (Table 3.4) were carried out. The experimental results (Fig. 5.10) show that both the liquid surface elevations and the base shear forces were reduced due to the increase of liquid viscosity. The nonlinearities of liquid sloshing becomes weakened when high-viscosity liquid is used. The TLD model proposed by the author is originally

Figure 5.10 Frequency response of wave surface elevation and base shear force of TLD.

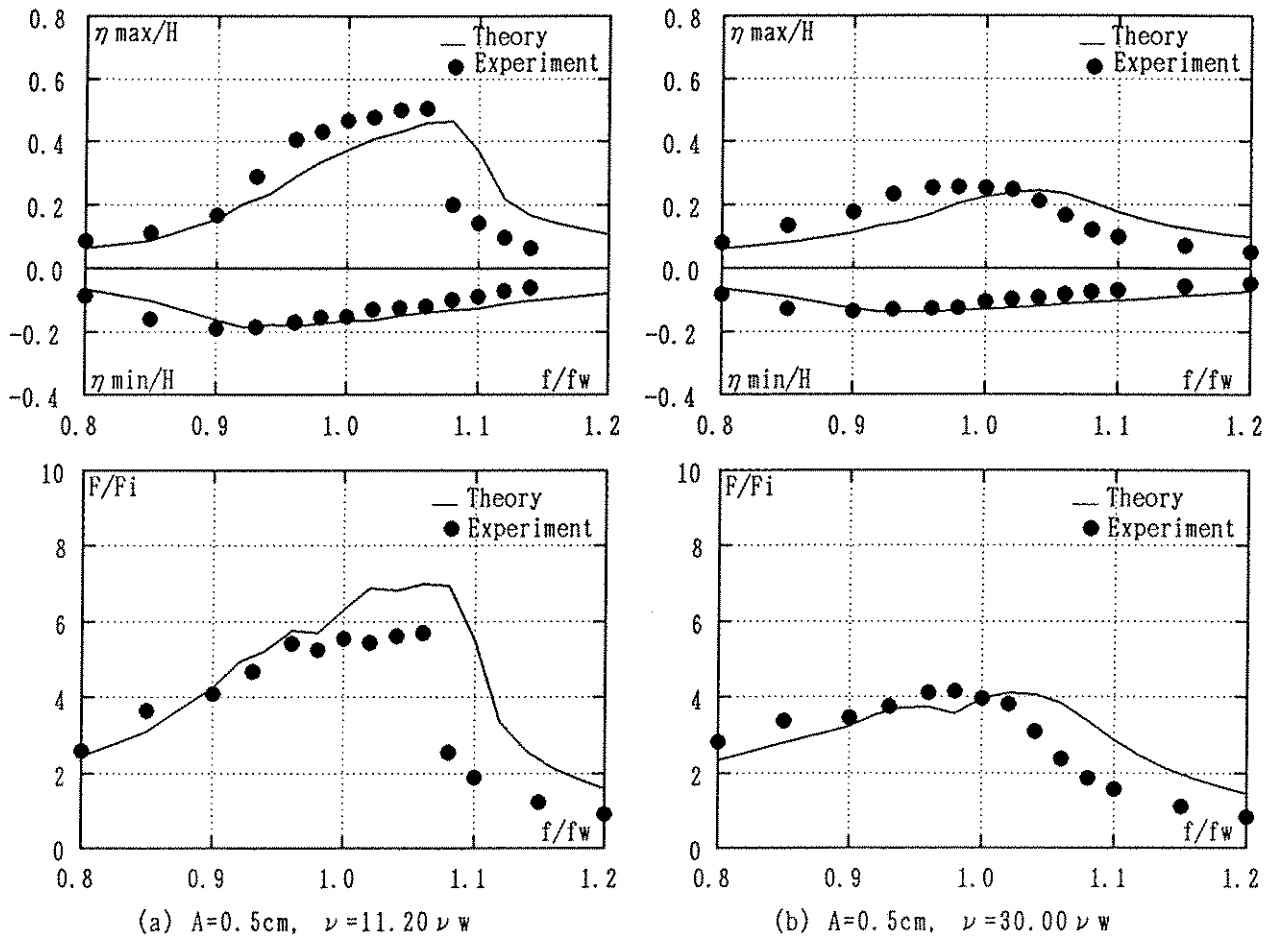

(a) A=0.5cm, ν=11.20ν_w (b) A=0.5cm, ν=30.00ν_w

for low-viscosity liquid such as water. To examine the applicability of the model for TLD with high-viscosity liquid, the simulations were carried out and the results are also shown in Fig. 5.10. Between the experimental results and the theoretical simulations, there are some discrepancy in the resonance frequency, but the overall agreement is good. Within all the experiment cases, it appears that the model can predict the motion of even high viscosity ($\nu=30\nu_w$). Effect of TLD with various liquid viscosity is also studied by the TLD-Structure Interaction simulation. Consider a SDOF structure ($f_s = 0.458Hz$, $\xi_s = 3.2\%$) subjected to a external force $Fe=F_o sin(2\pi ft)$ (F_o is constant) and its resonance amplitude without damper is assumed to be $1.0cm$. The liquid mass in TLD is 1% of the structure. The simulation results of the structural response with and without TLD are shown in Fig.5.11.

TLDs with liquid viscosity ν_w, $5\nu_w$ and $20\nu_w$, respectively, are used in the simulation. In all these cases, the maximum structural response decreases to less than $0.12cm$ after installing TLD. With low-viscosity liquid (ν_w), the frequency response curve has two distinct peaks around f/fw=0.95 and 1.05. Increasing liquid viscosity to $5\nu_w$, the local peak values of response curve decrease and the value at $f/f_w=1.00$ increases. Then the response curve becomes a one-peak curve when ν is further increased to $20\nu_w$. It appears that the optimal value of liquid viscosity is about $5\nu_w$ in this example.

Figure 5.11 The response of structure with TLD.

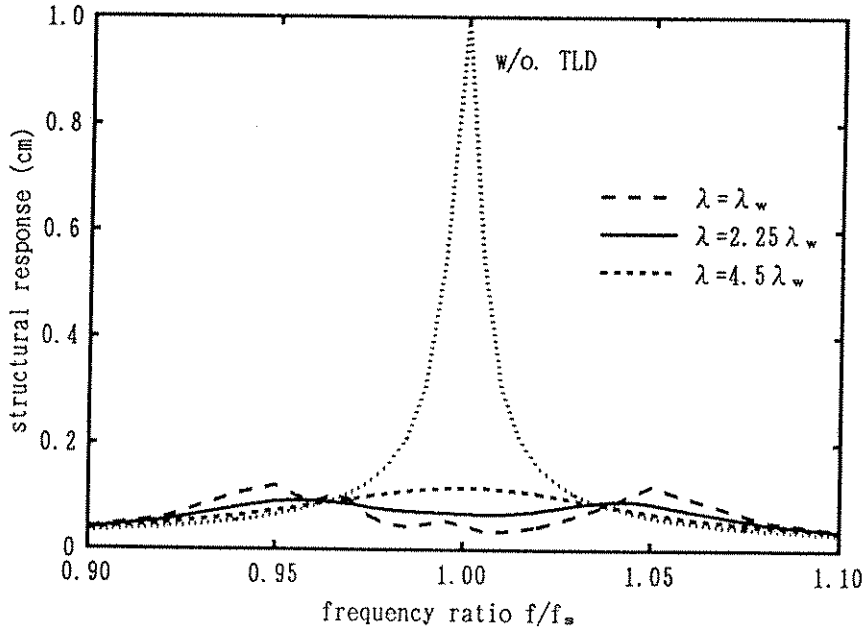

5.3.3 Increase of Damping of Liquid Sloshing by Floating Materials on Free Surface

The shaking table experiment of TLD with additional floating materials on the liquid free surface was carried out. The floating materials used in the experiment are expanded polystyrol balls and ploypropylene balls with their diameters of *2-5 mm*, which have special density less than *1.0 kg/cm³* so can float on the surface of water (Fig. ??). It is expected that the damping of liquid sloshing can be increased by the frictions on the free surface due to the floating materials.

An example is shown in Fig. 5.12. In this experiment case, the TLD tank size is *2a=39 cm*. water depth *h=6.0cm*, and the amplitude of a sinusoidal base motion is *0.1cm*. The wave amplitude was significantly reduced after expanded polystyrol balls with *500 cc* were added on the free surface of water. The nonlinearities of liquid sloshing were weakened also.

From the shaking table experiments by Nozawa [1990], it is found that the floating surface materials give a remarkable additional damping especially when liquid sloshing is in a small amplitude and the liquid depth is not so high ($\varepsilon<0.5$). A larger mount value of floating materials gives a higher additional damping.

Figure 5.12 Effect of floating materials on liquid damping.

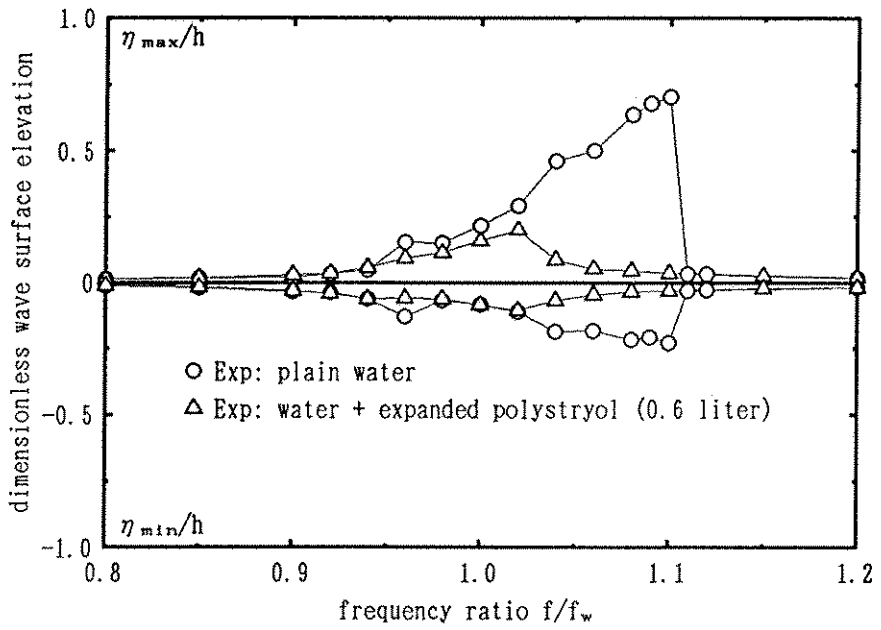

The TLD-structure interaction experiments using TLD with floating surface materials or with high-viscosity liquid were carried out [Fujino et al. 1990] (Fig. 5.13). The experiments show that the effectiveness of TLD can be improved by these means. In the experiments, 5 TLD's with tank size $2a=32.2cm$, $b=25.5cm$, water depth $h=3.4cm$ were used, corresponding to a mass ratio of 2.1%. The structure was under a sinusoidal excitation which caused a $1.0cm$ structural response amplitude at the resonance. The floating surface materials was $600\ cc$ expanded polystyrol balls. As a high-viscosity liquid, ethylene glycol was used, whose dynamic viscosity ν is about 16 times of that of water. The structural response with plain water TLD is also plotted for comparison in Fig. 5.13. As shown in Fig. 5.13, the maximum response amplitude of the structure is reduced by using high-viscosity liquid or adding floating surface materials.

Figure 5.13 TLD-structure response.

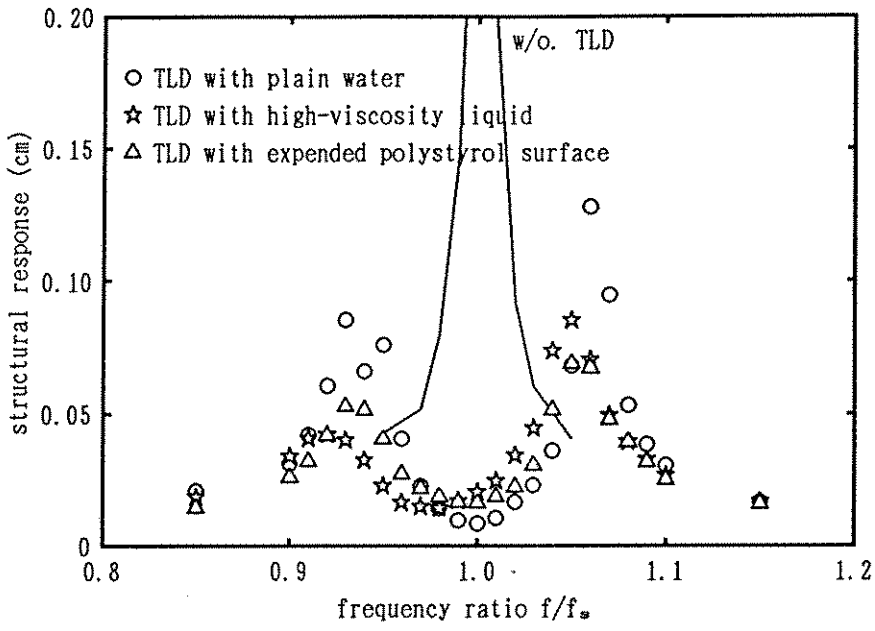

5.4 EMPIRICAL MODEL FOR DAMPING OF LIQUID SLOSHING DUE TO BREAKING WAVES

Several means increasing damping of liquid sloshing have been discussed in last section. Among those, utilizing of shallow liquid is one of the easy choices to

obtain high damping. However, waves in such a shallow-water TLD break in a relatively small base-motion. The model proposed in Chapter 2 which assumes the smooth liquid surface (i.e., no breaking waves) becomes invalid when breaking waves occur. The model is therefore modified by introducing two coefficients in the basic equations in order to account for breaking waves.

In this section, the determinations of two coefficients are presented in detail, and is examined by the TLD-structure interaction experiment.

5.4.1 Modified Basic Equations

The TLD model proposed in Chapter 2 may not be valid for the presence of wave breaking situation because of the assumption of free surface continuity. To account for breaking waves in the TLD model, the equation of motion (Eq.(2.42)) was modified by introducing two coefficients, C_{da} and C_{fr} as follows,

$$\frac{\partial}{\partial t}u(\eta) + (1\text{-}T_H^2)\,u(\eta)\frac{\partial}{\partial x}u(\eta) + C_{fr}^2\, g\frac{\partial \eta}{\partial x} + gh\sigma\phi\frac{\partial^2\eta}{\partial x^2}\frac{\partial \eta}{\partial x} = -C_{da}\lambda u(\eta) - \ddot{x}_s. \quad (5.12)$$

Those coefficients are unity when breaking waves do not exist. Referring to the definition of breaking waves in coastal engineering, the critical condition for breaking waves in this study is defined as that wave height is larger than liquid depth h.

5.4.2 Coefficients C_{da} and C_{fr} and Their Identifications from Experiment

When waves break, large energy is dissipated on the liquid free surface, resulting in that liquid sloshing has high damping. C_{da}, therefore, was introduced in Eq.(5.12) to modify the liquid damping, and is called as a damping coefficient. On the other hand, wave breaking also change correspondingly the wave phase velocity. So, C_{fr} was introduced into Eq.(5.12) to modify the phase velocity. Since the change of wave phase velocity also reflects the shift of the natural frequency of liquid sloshing, C_{fr} is called as a frequency shift coefficient.

Values of these two empirical coefficients were identified by the sweep harmonic shaking table experiment. Energy dissipation per cycle (Eq.(4.3)) can be computed from the measurements of experiment as discussed in Section 4.1. This quantity was chosen as a reference to identify the coefficients C_{da} and C_{fr},

An example is shown in Fig. 5.14; a trial-and-error approach was adopted to minimize the error between experimental results and simulation results which are calculated by the modified TLD model. Four experimental cases (Table 3.2) with various TLD tank size and liquid depth have been carried out for the identification of C_{da} and C_{fr}. The details are given in Appendix E. It is found that C_{da} is dependent upon the base amplitude, A, while C_{fr} almost takes a constant of *1.05* for the four experimental cases. After nondimensionalizing Eq. (5.12), the coefficients in the damping term and in the forcing term ($\ddot{x}_s$) indicate the following functional relationship;

$$\frac{C_{da}\sqrt{\omega_w \nu}}{\varepsilon\sqrt{g h}} = \Pi\left(\frac{\omega_w^2 A}{\varepsilon g}\right), \tag{5.13}$$

where Π is a function. On this basis, value of C_{da} identified experimentally are plotted in Fig. 5.15. The function is determined by the method of least squares and is obtained as

$$C_{da} = 0.57\sqrt{\frac{\varepsilon h\ \omega_w}{\nu} A}, \tag{5.14}$$

where $\omega_w = 2\pi f_w$ is the angular fundamental natural frequency of liquid sloshing.

5.4.3 Comparison with Experiments and Discussions

Figure 5.16 shows TLD-structure interaction results under large external forces. In these experiments, breaking waves in TLD were clearly observed around the resonance. The TLD tank used here is *39.0 cm* in length and filled with *3.0 cm* water, which has a natural sloshing frequency tuned to the structural natural frequency, f_s=*0.689 Hz*. The mass ratio of TLD to the structure is *1.05 %*. The resonant amplitude of structural response without TLD is *5.0 cm* for the case shown in Fig. 5.17a, and *10.0 cm* for that in Fig. 5.16b, respectively. In Fig. 5.16, the structural response predicted by the modified TLD model is also given. In the simulation, C_{fr}=*1.05* and Eq.(5.14) for C_{da} were used when the wave height near the end wall of TLD tank exceeds the water depth h. The modified model noticeably improves prediction accuracy (Fig. 5.16a) and satisfactory agreement between experiment and simulation can be seen (Fig.5.16a and 5.16b).

Figure 5.14 Example of determination of C_{do} and C_{ff} by energy dissipation per cycle.

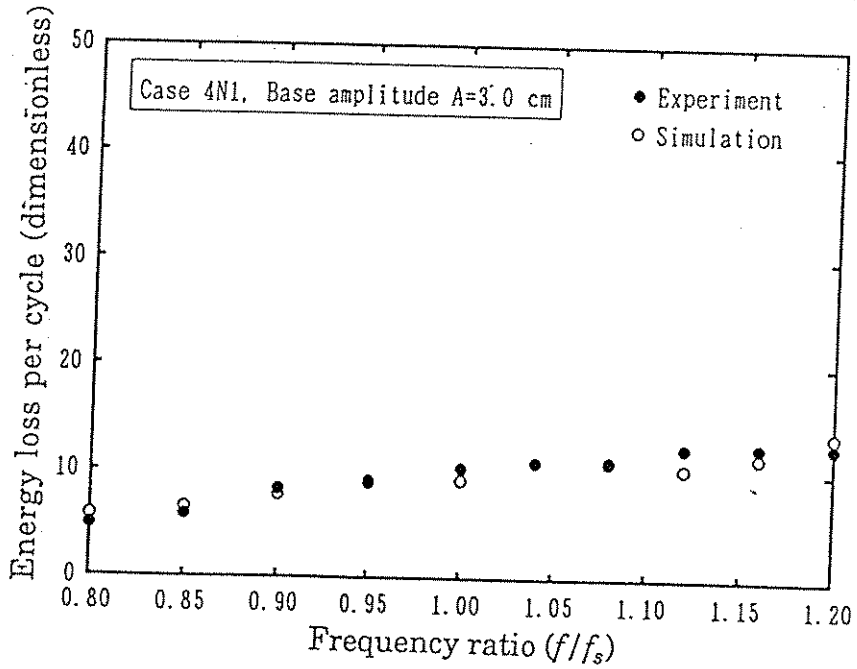

Figure 5.15 The relation between the damping term and the forcing term.

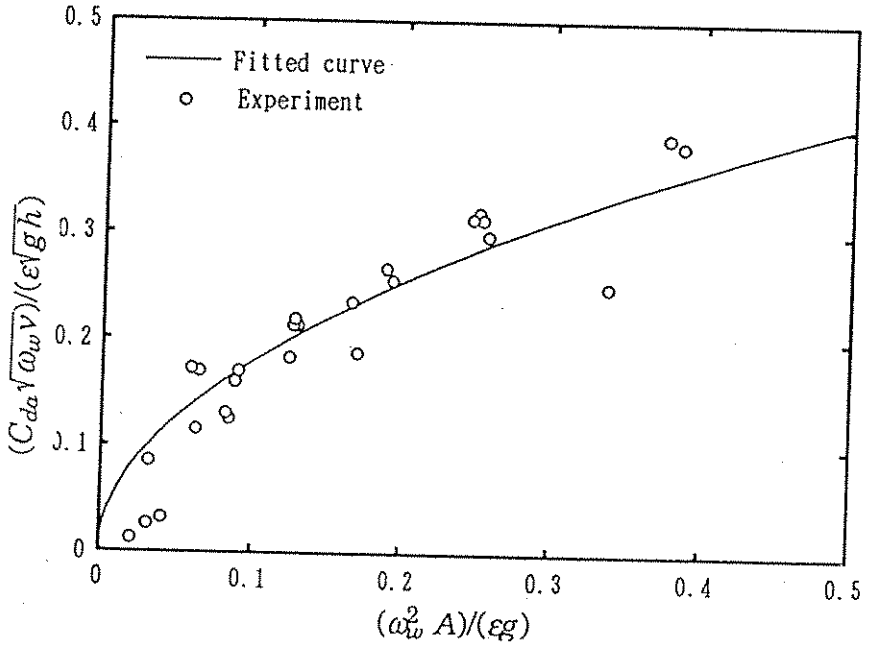

Figure 5.16a The response of structure with TLD (X_o=5.0cm).

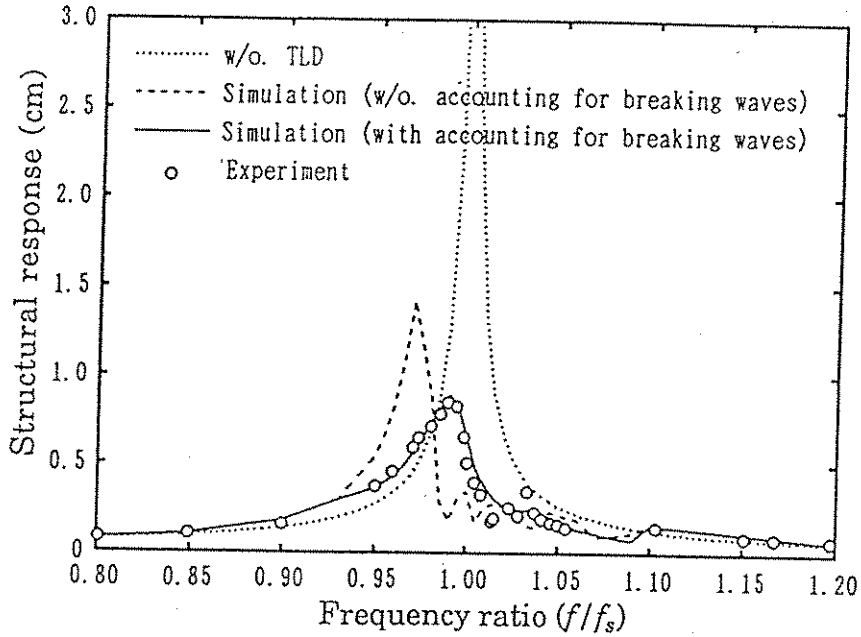

Figure 5.16b The response of structure with TLD (X_o=10.0cm).